



Aalborg Universitet

AALBORG UNIVERSITY
DENMARK

Full-Scale Tests on Loaded Glulam Beams with Square Cross-Section Exposed to Parametric Fire on Four Sides

Hansen, F. Toft; Olesen, Frits Bolonius

Publication date:
1996

Document Version
Publisher's PDF, also known as Version of record

[Link to publication from Aalborg University](#)

Citation for published version (APA):
Hansen, F. T., & Olesen, F. B. (1996). *Full-Scale Tests on Loaded Glulam Beams with Square Cross-Section Exposed to Parametric Fire on Four Sides*. Dept. of Building Technology and Structural Engineering, Aalborg University. R / Institut for Bygningsteknik No. R9617

General rights

Copyright and moral rights for the publications made accessible in the public portal are retained by the authors and/or other copyright owners and it is a condition of accessing publications that users recognise and abide by the legal requirements associated with these rights.

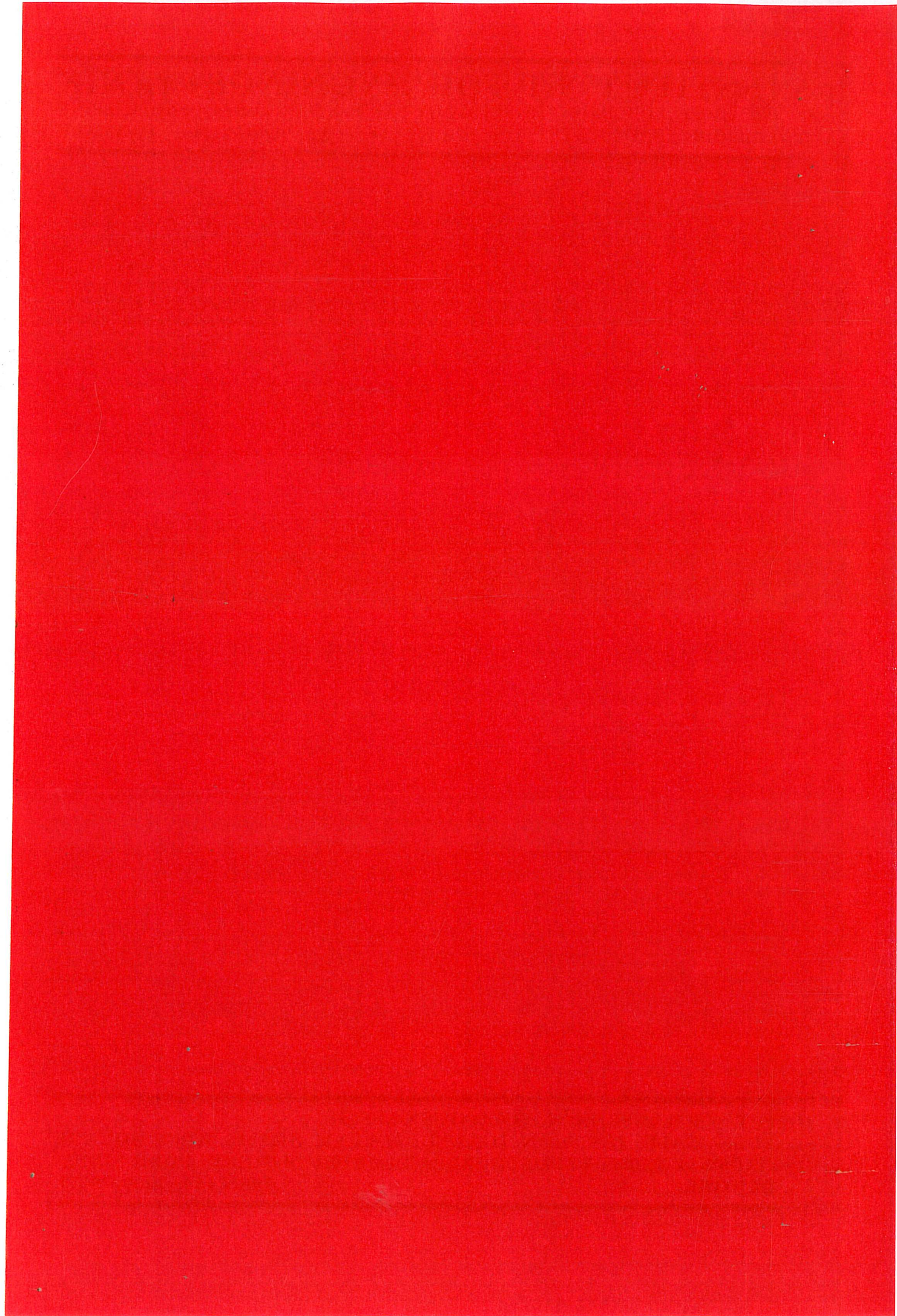
- Users may download and print one copy of any publication from the public portal for the purpose of private study or research.
- You may not further distribute the material or use it for any profit-making activity or commercial gain
- You may freely distribute the URL identifying the publication in the public portal -

Take down policy

If you believe that this document breaches copyright please contact us at vbn@aub.aau.dk providing details, and we will remove access to the work immediately and investigate your claim.

INSTITUTTET FOR BYGNINGSTEKNIK
DEPT. OF BUILDING TECHNOLOGY AND STRUCTURAL ENGINEERING
AALBORG UNIVERSITET • AAU • AALBORG • DANMARK

F. TOFT HANSEN & F. BOLONIUS OLESEN
FULL-SCALE TESTS ON LOADED GLULAM BEAMS WITH SQUARE
CROSS-SECTION EXPOSED TO PARAMETRIC FIRE ON FOUR SIDES
OCTOBER 1996 **ISSN 1395-7953 R9617**



INSTITUTTET FOR BYGNINGSTEKNIK

DEPT. OF BUILDING TECHNOLOGY AND STRUCTURAL ENGINEERING
AALBORG UNIVERSITET • AAU • AALBORG • DANMARK

F. TOFT HANSEN & F. BOLONIUS OLESEN
FULL-SCALE TESTS ON LOADED GLULAM BEAMS WITH SQUARE
CROSS-SECTION EXPOSED TO PARAMETRIC FIRE ON FOUR SIDES
OCTOBER 1996 **ISSN 1395-7953 R9617**

PREFACE

The present report contains the preliminary test results of a supplementary series of experimental investigations performed in 1993/94 into the charring, load-bearing and deformation properties of loaded glued laminated beams exposed to parametric fire.

The full-scale tests and the material tests are the second stage in a more extensive theoretical and experimental investigation of the performance of glued laminated structures subject to fire exposure. Where the first series of tests, performed in 1987/88 and reported in ISSN 0902-7513 R 9223, dealt with specimens of "normal" beam-sections, this second series deals with beams of approximately square-shaped cross-section, aiming at analysis of timber columns.

The test results are published separately in the present form without explanation of the analytical treatment of the problem. This has been done to make the test results available to interested colleagues at the earliest possible state, especially with a view to the work being performed these years on adjusting the national codes of practice to Eurocode 5.

Aalborg, October 1996

F.Toft Hansen

F.Bolonijs Olesen

FULL-SCALE TESTS ON LOADED GLULAM BEAMS WITH SQUARE CROSS-SECTION EXPOSED TO PARAMETRIC FIRE ON FOUR SIDES

F. Toft Hansen & F. Bolonius Olesen
Aalborg University

Introduction

Eurocode 5: Design of Timber Structures includes a part 1-2: General rules - Structural fire design (ENV 1995-1-2, november 1994). As is the case with the Eurocode-complex in general, this part of the code is primarily based on the concept of standard fire exposure, according to ISO 834. However, part 1-2 also gives principles for a more differentiated structural fire design, e.g. based on the concept of parametric fire exposure, i.e. fire exposure including both a period of increasing temperature and a subsequent period of cooling, determined by the fire load, the ventilation properties and the thermal properties of the fire compartment as the governing parameters.

This concept of structural fire design, of course, requires more differentiated rules and approximations with respect to charring rates, material properties and structural response than the simplified concept of standard fire design. Some of the background material for this are wellknown facts, but due to the lack of sufficient information, supplementary investigations have been carried out in recent years. A contribution to this pre-normative work is a series of full-scale tests with parametric fire exposure on loaded glulam beams, performed in the structural fire laboratory at Aalborg University in 1987/88 (referred by F. Toft Hansen & F. Bolonius Olesen in Report ISSN 0902-7513 R9223, Aalborg University, september 1992).

From these investigations it was observed that the internal temperatures in the specimens still increased for a long period after the charring process had stopped, and that the same was the case - to an even greater extent - with the deflections of the beams. This seems to indicate that creep effects at elevated temperatures (100-300 °C) in timber structures have much greater influence on the deformation properties than noticed so far. At any rate the deformations measured were significantly larger than what could be expected by calculation in accordance with the design rules used so far in most countries. Obviously, this is of great importance for the fire design of timber columns, which might give rise to the question, if the rules used so far for design of slender timber structures are on the safe side.

To elucidate this problem, a series of full-scale fire tests on loaded glulam beams exposed to parametric fire has been performed in the fire laboratory in 1993/94. The investigations followed the same guidelines as the tests performed earlier, but especially aiming at design of timber columns, specimens with approximately square-shaped cross-section exposed on all four sides have been tested. The test programme has been extended essentially, especially with respect to registration of the strength and stiffness properties of the materials.

This report is the first part of the documentation of the investigations. It contains a description of the test programme and the test procedures, as well as the results of the material tests and the full-scale tests. The second part (in preparation) will contain the analysis of the test results and the conclusions that can be drawn from the investigations.

1. Test specimens

For the fire test, 2x8 specimens of glulam beams were performed.

8 specimens with the dimensions 160·200·4500 mm

8 specimens with the dimensions 185·200·4500 mm

all with the humidity $\omega=0.080-0.095$.

The numbering of beams with the cross-sectional area 160·200 mm was:

$_{122}^1$ $_{324}^1$ $_{526}^1$ $_{728}^1$

$_{142}^3$ $_{344}^3$ $_{546}^3$ $_{748}^3$

and for beams with the cross-sectional area 185·200 mm:

$_{162}^5$ $_{364}^5$ $_{566}^5$ $_{768}^5$

$_{182}^7$ $_{384}^7$ $_{586}^7$ $_{788}^7$

For a cutting as shown in figure 1 below, the number $_{324}^1$ signifies a beam number 24 with the length $l = 3200$ mm in the middle and 2 parts, number 32 and 41, at the ends.

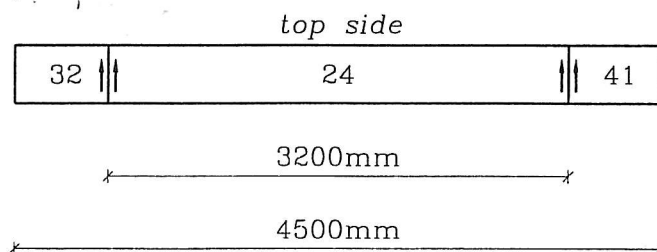


Figure 1 Cutting of the beams.

2. Mechanical properties

2.1 Bending tests

The modulus of elasticity in static bending (E) was determined for all beams, numbers 22 - 88. The shear modulus (G) was also determined but the result was useless, i.e. values between 150 and 250 Mpa.

2.2 Tension and compression tests parallel to the grain

Specimens for tension and compression tests were taken from the cut-off ends, e.g. from no. 32, (cf. figure 2.2.1).

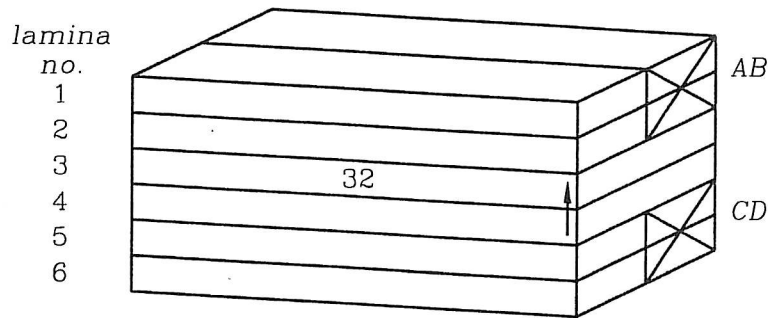


Figure 2.2.1 Specimen no. 32.

Specimens for tension tests were cut from the single lamina, i.e. from no.1 and no.2 and also no.5 and no.6. The number of the specimens could then be no.321 or no.325. Figure 2.2.2 shows the specimens for tension tests.

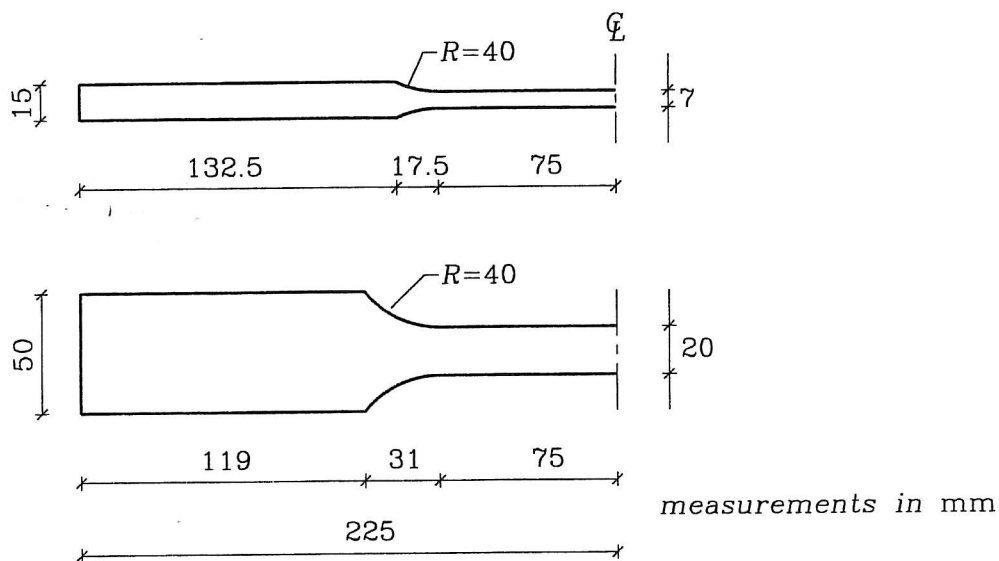


Figure 2.2.2 Specimens for tension test parallel to the grain.

Specimens for compression tests were cut from 2 laminae, i.e. from no.AB or no.CD. The number of the specimens could then be no.32AB or no.32CD. The dimension of the specimens was 40·40·120 mm.

For each test specimen, the modulus of elasticity in tension/compression was determined as well as the ultimate strength.

The results of the modulus of elasticity are shown in table 2.1.

The results of the test of the ultimate strength in tension/compression are shown in table 2.2, where $f_t = F_u/A$ = tension strength and $f_c = F_u/A$ = compression strength. F_u = ultimate load, A = cross - sectional area.

Beam no.	Lamina no.		Modulus of elasticity (E) [MPa]			comments
	compress.	tension	bending	compress.	tension	
22	12AB 12CD	211 212 215 216	17110	10033 12570	10395 12285 15120 9685	
24	32AB 32CD	411 412 415 416	16329	9669 17345	11960 -- 10933 14255	
26	52AB 52CD	611 612 615 616	16907	12025 13305	11005 10690 12930 9874	
28	72AB 72CD	811 812 815 816	18359	15700 15335	11800 9682 10979 15505	
42	14AB 14CD	231 232 235 236	17037	9965 12985	7552 11405 12755 11220	
44	34AB 34CD	431 432 435 436	15435	15125 12555	9930 10455 10199 8569	
46	54AB 54CD	631 632 635 636	15946	10180 12910	7103 8080 14155 8724	
48	74AB 74CD	831 832 835 836	17396	19000 10860	9759 13440 6260 11100	
62	25AB 25CD	251 252 255 256	17660	5953 6569	13685 9420 9889 10058	

Table 2.1 Mechanical properties. Modulus of elasticity.

Beam no.	Lamina no.		Modulus of elasticity (E) [MPa]			comments
	compress.	tension	bending	compress.	tension	
64	36AB	451	16876	12185	13175	
		452			11300	
	45CD	455			7180	
		456			14755	
66	65AB	651	17242	8718	8922	
		652			11859	
	65CD	655			11185	
		656			10735	
68	85AB	851	17662	9373	14155	
		852			7885	
	76CD	855			11780	
		856			9645	
82	27AB	271	15775	9232	12675	
		272			9765	
	18CD	275			13350	
		276			--	
84	47AB	471	16058	12550	13350	
		472			11265	
	47CD	475			12975	
		476			12220	
86	67AB	671	15551	6984	12025	
		672			9357	
	58CD	675			11970	
		676			6716	
88	78AB	871	18069	13345	16160	
		872			10100	
	87CD	875			14935	
		876			10372	

Table 2.1 Mechanical properties. Modulus of elasticity.

Beam no.	Lamina no.		Strength in MPa		comments
	compress.	tension	compress.	tension	
22	12AB	211	36.5	73.7	
		212		80.3	
	12CD	215	47.8	71.5	
		216		47.8	
24	32AB	411	40.7	50.6	
		412		--	
	32CD	415	51.9	64.1	
		416		81.7	
26	52AB	611	48.3	71.2	failure at knot
		612		52.6	
	52CD	615	51.0	88.8	
		616		44.3	
28	72AB	811	49.6	44.2	
		812		55.5	
	72CD	815	55.5	59.9	
		816		89.4	
42	14AB	231	42.0	48.6	
		232		80.0	
	14CD	235	53.5	101.6	
		236		90.2	
44	34AB	431	55.5	44.0	failure at knot failure at knot
		432		34.7	
	34CD	435	45.5	46.0	
		436		58.2	
46	54AB	631	42.1	26.3	failure at knot
		632		49.1	
	54CD	635	46.4	75.1	
		636		74.6	
48	74AB	831	59.3	78.9	
		832		103.9	
	74CD	835	42.0	46.1	
		836		82.1	
62	25AB	251	39.6	93.1	
		252		64.0	
	25CD	255	40.6	69.0	
		256		56.2	

Table 2.2 Mechanical properties. Compression and tension strength.

Beam no.	Lamina no.		Strength in MPa		comments
	compress.	tension	compress.	tension	
64	36AB	451	45.7	54.2	
		452		67.5	
	45CD	455	41.4	57.6	
		456		105.1	
66	65AB	651	40.2	62.8	
		652		55.8	
	65CD	655	42.9	90.1	
		656		83.6	
68	85AB	851	40.3	88.2	
		852		47.5	
	76CD	855	41.6	83.2	
		856		58.0	
82	27AB	271	38.9	82.1	big annual rings
		272		84.3	
	18CD	275	46.0	93.3	
		276		30.5	
84	47AB	471	41.3	73.6	
		472		74.7	
	47CD	475	43.8	59.3	
		476		77.6	
86	67AB	671	36.0	64.5	
		672		75.6	
	58CD	675	41.2	74.1	
		676		57.8	
88	78AB	871	48.5	109.0	
		872		53.2	
	87CD	875	44.2	79.4	
		876		50.1	

Table 2.2 Mechanical properties. Compression and tension strength.

3. Fire test of beams

3.1 Test set-up

The Fire Research Laboratory at the Department of Building Technology and Structural Engineering comprises 3 different furnaces for testing of load-bearing structures under and after fire-exposure. Described by N.J.Hviid & F.Boloniussen in Report R 7801, Aalborg University, march 1978. The furnace of the load equipment for beams was given the inner dimensions 1600·1600·2200 mm. The furnace was heated by 6 gas burners inserted at the bottom of the furnace.

The mechanical load equipment placed outside the furnace comprises two vertical portal frames. At the two ends of the furnace, the test beams were simply supported and above the furnace, 2 load cells of 200 kN each for vertical loads were mounted as well as 4 transducers for measuring vertical deflections (cf. figure 3.1.1).

From the load cell the force P was transmitted to the test beam through a water-cooled steel column. In a similar way, a quartz tube linked the transducer to the test beam.

The temperature inside the furnace was measured by means of NiCr-Ni thermo couples.

During the fire test the heat inside the furnace was manually controlled by a Chino 6-channel recorder. All the measured data were recorded by a Fluke-Datalogger and stored on a Logfile.

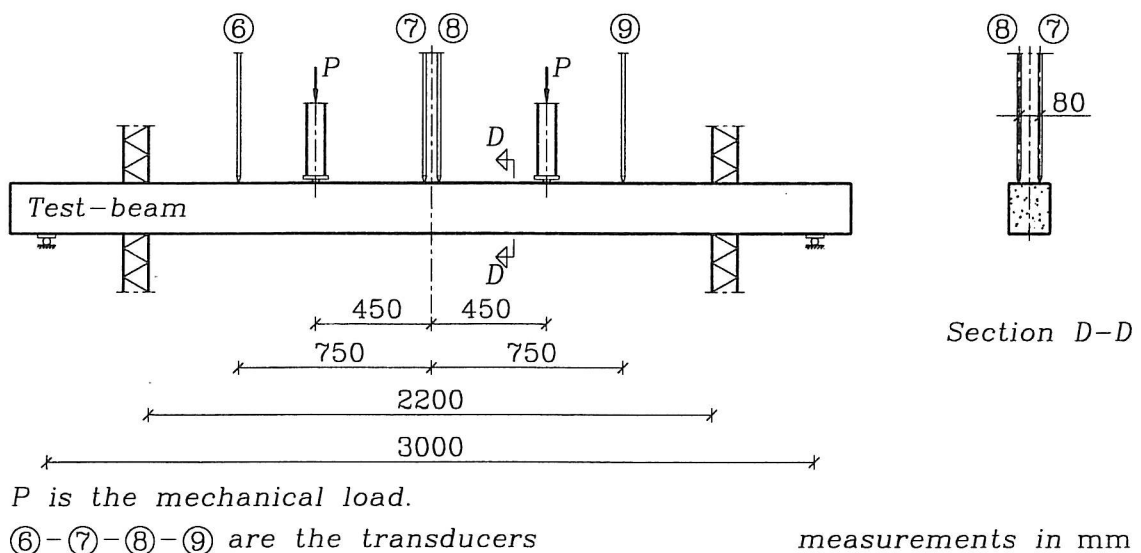


Figure 3.1.1 Test set-up.

3.2 Test procedure

The mechanical load was applied prior to the fire test. For beams with the width $b = 160$ mm the load was 2·1.6 kN and for beams with the width $b = 185$ mm the load was 2·2.2 kN. One single beam (G44) had a different load (2·2.0 kN).

6 different combinations of the opening factor (F) and the fire load density (q_f) were chosen as thermal fire load.

The 6 combinations were:

$F \text{ (m}^{1/2}\text{)} / q_t \text{ (MJ/m}^2\text{)}$
 0.04 / 126
 0.04 / 188
 0.06 / 113
 0.06 / 188
 0.08 / 151
 0.08 / 251

During the fire exposure the mechanical load was maintained either until bending failure in the beam occurred, or the temperature inside the furnace had decreased to about 300°C. After that, the mechanical load was increased until bending failure in the beam occurred.

During the entire fire exposure, temperatures and corresponding values of vertical beam deflections were measured.

3.3 Test results

The direct results of the fire tests are specified in table 3.3.1.

Beam no.	Mechanical load (P) kN	Ultimate load (P_{ult}) kN	Thermal load		Time to failure min.
			$F \text{ (m}^{1/2}\text{)}$	$q_t \text{ (MJ/m}^2\text{)}$	
GL 26	2 · 1.6	2 · 3.4	0.04	126	87
GL 46	2 · 1.6	2 · 1.6	0.04	188	79
GL 28	2 · 1.6	2 · 6.4	0.06	113	58
GL 24	2 · 1.6	2 · 2.9	0.06	188	85
GL 42	2 · 1.6	2 · 4.7	0.08	151	61
GL 62	2 · 1.6	2 · 1.6	0.08	251	62
*) GL 44	2 · 2.0	2 · 2.0	0.06	188	74
GL 82	2 · 2.2	2 · 4.7	0.04	126	87
GL 84	2 · 2.2	2 · 2.2	0.04	188	106
GL 86	2 · 2.2	2 · 8.9	0.06	113	51
GL 88	2 · 2.2	2 · 3.9	0.06	188	87
GL 66	2 · 2.2	2 · 6.7	0.08	151	51
GL 68	2 · 2.2	2 · 3.5	0.08	251	88

*) GL 62 was reduced to the width $b = 160 \text{ mm}$ because the fire test failed for GL 22 and GL 48.

Table 3.31 Test results. Ultimate loads.

Graphs of the thermal fire load and the vertical deflection of the beams as a function of the temperature/time are shown in annex 1.

As an example the graph for the beam no. GL 44 is shown in figure 3.31.

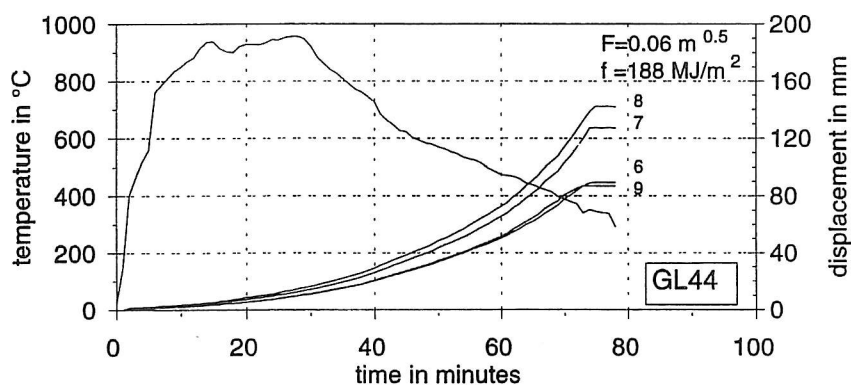


Figure 3.3.1 GL 44. Thermal fire load and displacements at the points 6,7, 8 and 9.

Furthermore, the residual cross - sectional area of the beams in three different sections A, B and C have been determined (cf. annex 2). Their location is shown in figure 3.3.2.

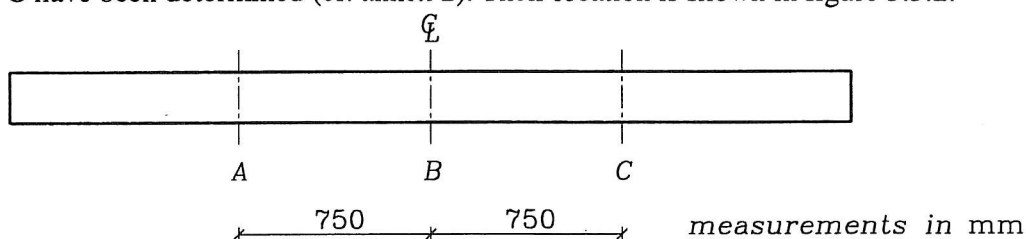


Figure 3.3.2 Location of the sections A, B and C.

As an example, the cross-section A before and after fire exposure, is shown for beam GL 44 in figure 3.3.3.

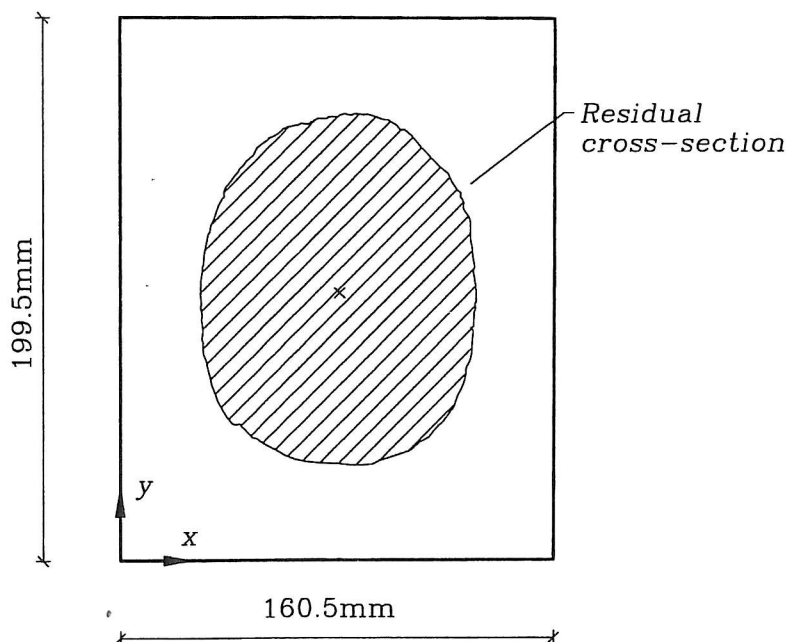


Figure 3.3.3 The beam GL44, cross-section A, before and after fire exposure.

In the table 3.3.2 below, the residual cross-sectional area and the principal moments I_1 and I_2 belonging to cross-section A, B and C for all the beams are stated.

Beam no.	Fire load F/q_t	cross-section no.	Area mm^2	Principal moments		x - y directions about centroid
				$I_1 [\text{mm}^4]$	$I_2 [\text{mm}^4]$	
GL26	0.04/126	A	10250	10,335,748	6,793,112	0.995946/-0.089948
		B	11890	13,927,831	9,134,308	0.999999/ 0.000361
		C	11676	14,425,999	8,186,085	0.999650/-0.026452
GL46	0.04/188	A	8319	7,551,215	4,035,617	0.999453/-0.033076
		B	8871	8,160,742	4,864,943	0.999750/ 0.022378
		C	8520	7,738,193	4,346,708	0.998449/ 0.055674
GL28	0.06/113	A	18100	36,137,422	19,404,042	0.997854/ 0.065477
		B	17808	34,921,837	18,735,247	0.999993/-0.003687
		C	18219	35,777,362	19,963,033	0.999995/ 0.003146
GL24	0.06/188	A	10622	11,365,290	7,117,477	0.999366/-0.035602
		B	9882	10,600,153	5,724,840	0.999973/-0.007312
		C	10488	11,521,167	6,682,147	0.999989/-0.004631
GL42	0.08/151	A	14792	22,449,697	13,683,146	0.999762/-0.021815
		B	14114	22,023,204	11,779,375	0.999350/ 0.036065
		C	13934	19,805,910	12,154,429	0.997424/-0.071737
GL62	0.08/251	A	8218	7,823,608	3,711,252	0.999278/ 0.038001
		B	8091	7,389,264	3,685,021	0.999967/ 0.008080
		C	8508	8,286,657	4,057,934	0.999163/ 0.040914
GL44	0.06/188	A	9545	9,150,854	5,769,618	0.995420/ 0.095602
		B	10794	12,892,352	6,737,084	0.998829/ 0.048377
		C	10521	11,848,827	6,573,547	0.999039/-0.043831
GL82	0.04/126	A	17178	27,561,359	20,215,869	0.994986/ 0.100014
		B	16566	24,754,202	19,474,321	0.998191/-0.060121
		C	16389	25,475,995	18,051,390	0.999999/ 0.001576
GL84	0.04/188	A	10694	10,272,706	8,089,034	0.997199/ 0.074790
		B	11085	11,329,060	8,478,093	0.981492/-0.191502
		C	10572	10,105,351	7,851,462	0.999124/-0.041843
GL86	0.06/113	A	20703	38,250,404	31,485,949	0.992300/ 0.123856
		B	20771	38,960,765	31,347,433	0.999889/-0.014919
		C	19932	34,856,078	29,424,249	0.977531/-0.210792
GL88	0.06/188	A	14199	18,714,461	13,860,454	0.998815/-0.048665
		B	13140	16,548,632	11,505,292	0.992712/ 0.120514
		C	13163	16,899,391	12,013,725	0.999145/-0.041337
GL66	0.08/151	A	18643	31,424,230	25,086,700	0.998175/ 0.003867
		B	17519	26,883,546	23,025,112	0.994352/-0.106134
		C	18529	29,655,474	25,967,784	0.995526/ 0.094484
GL68	0.08/251	A	11943	12,340,284	10,507,519	0.971499/-0.237045
		B	11209	11,411,376	8,806,443	0.991731/-0.128332
		C	12293	14,200,682	10,223,234	0.980833/-0.194850

Table 3.3.2 Residual cross-sectional properties after fire exposure.

Based on the values of ultimate loads for the beams (cf. table 3.3.1) and the residual cross-sections after fire exposure (cf. table 3.3.2) the ultimate bending moment M_{ult} and the formal ultimate bending stress in tension σ_{ult}^f for each test beam can be approximately calculated by

$$\sigma_{ult}^f = M_{ult} \cdot y_f / I_f$$

where $M_{ult} = P_{ult} \cdot 1.05 \text{ kNm}$ (cf. figure 3.1.1),

I_f is the principal moment of inertia I_1 in the cross-section of failure,

y_f is the corresponding distance from the centroid to the bottom side.

As the position of the failure within the distance of maximum bending moment (0.90 m) cannot be determined exactly, the values of I_f and y_f in the cross-section of failure have been estimated from the known values of I_1 and y_1 in the cross-sections A, B and C (cf. figure 3.3.2), in the following way:

If $I_B/y_B < I_A/y_A$ and I_C/y_C , then I_f/y_f is put equal to I_B/y_B . If $I_B/y_B > I_A/y_A$ and/or I_C/y_C , then I_f/y_f is found by linear interpolation between I_B/y_B and the minimum value of I_A/y_A and I_C/y_C , i.e.

$$I_f/y_f = I_B/y_B - 0.45/0.75 \cdot (I_B/y_B - (I/y)_{\min}), \text{ cf. figure 3.1.1.}$$

The measured values of y_A , y_B and y_C and the calculated values of M_{ult} and σ_{ult}^f are shown in table 3.3.3.

Beam no.	M_{ult} kNm	y_A mm	y_B mm	y_C mm	σ_{ult}^f N/mm ²
GL26	3.570	64	67	71	19.8
GL46	1.680	59	56	57	12.7
GL28	6.720	84	83	84	16.0
GL24	3.045	63	64	64	18.3
GL42	4.935	74	75	72	17.3
GL62	1.680	62	61	61	13.9
GL44	2.100	61	68	66	12.7
GL82	4.935	77	77	77	15.4
GL84	2.310	60	63	60	12.5
GL86	9.345	82	79	82	20.7
GL88	4.095	70	69	69	17.1
GL66	7.035	75	75	73	19.7
GL68	3.675	63	63	66	20.3

Table 3.3.3 Ultimate bending moment and bending stress.

4. Temperature measuring inside the beams

During the entire fire exposure the temperatures inside the furnace as well as inside the beams were measured. For technical reasons, temperature measuring was carried out by means of a separate test set-up.

4.1 Test specimens and test programme

The intact beam ends after the fire test of the beams were taken as test specimens. By each set-up 2 specimens were tested. One specimen with the width $b = 160$ mm and one with the width $b = 185$ mm. Using the thermal fire load as a guide the programme was as follows:

$b = 160$ mm	←	fire load	→	$b = 185$ mm
GL26 a } GL26 b }	←	0.04/126	→	{ GL82 a { GL82 b
GL46 a } GL46 b }	←	0.04/188	→	{ GL84 a { GL84 a
GL28 a } GL28 b }	←	0.06/113	→	{ GL86 a { GL86 b
GL24 a } GL24 b }	←	0.06/188	→	{ GL88 a { GL88 b
GL42 a } GL42 b }	←	0.08/151	→	{ GL66 a { GL66 b
GL62 a } GL62 b }	←	0.08/251	→	{ GL68 a { GL68 b

4.2 Test set-up

The specimens with the length $l = 300$ mm were bolted to the walls inside the furnace in such a way that the thermo couples passing through the wall and the glulam beam end could be taken directly from the outside room temperature to the measuring points (cf. figure 4.1).

8 measuring points were placed inside each test specimen in the same cross-section. The number and the intended location of the measuring points in beams with the width $b = 160$ mm and beams with the width $b = 185$ mm are shown in the figure 4.2.

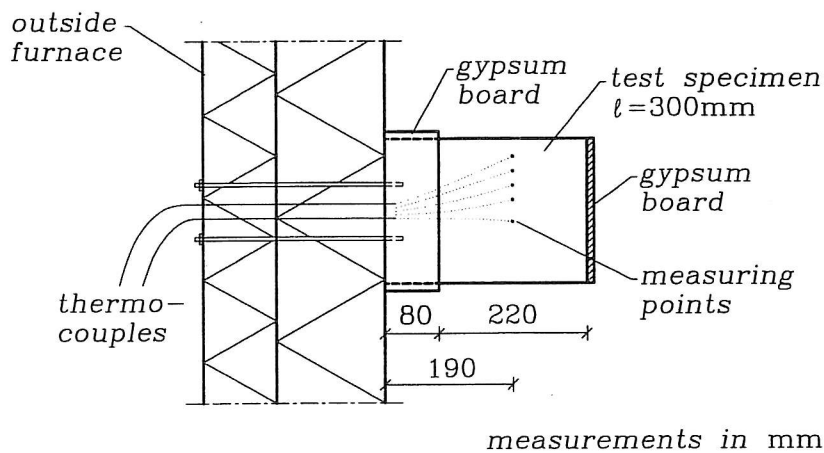


Figure 4.1 Test set-up.

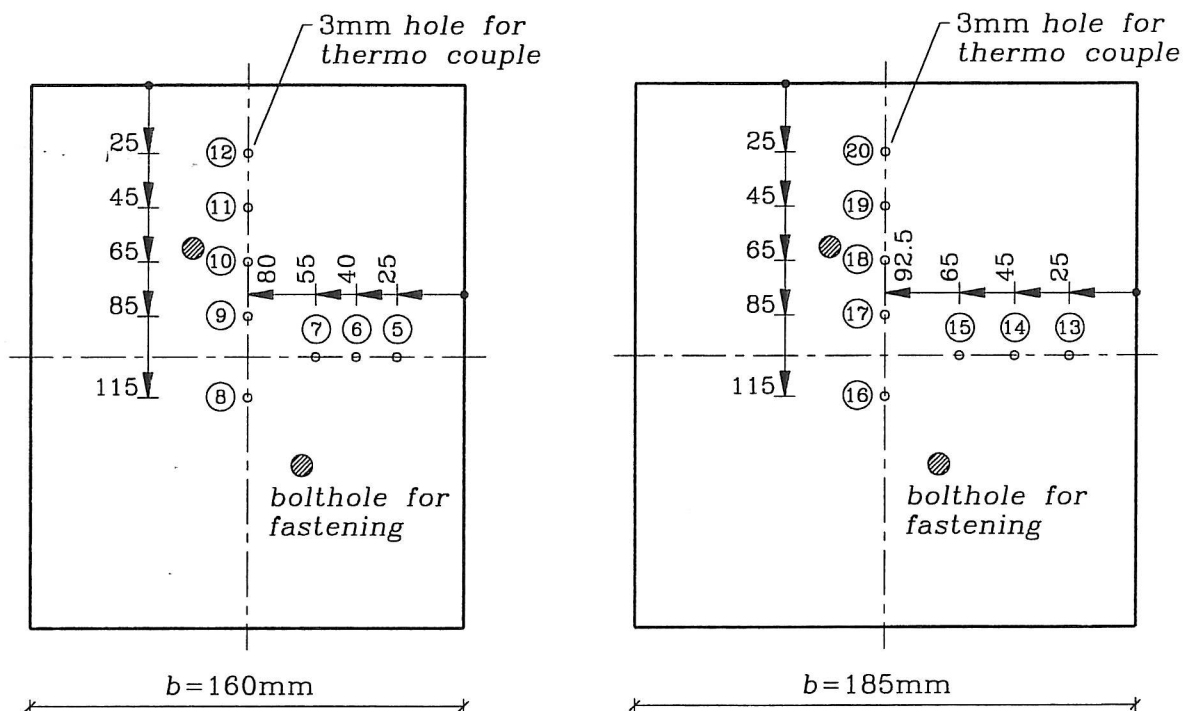


Figure 4.2 Intended measuring points in beams with the width $b = 160\text{ mm}$ and $b = 185\text{ mm}$.

4.3 Test procedure

For the thermal fire load as shown in part 4.1 the same 6 combinations as used for the beams in part 3 were used. The fire load was interrupted when the temperature inside the furnace was reduced to about $300\text{ }^{\circ}\text{C}$. A few tests were continued after that to follow the temperature development inside the beams.

4.4 Test results

The test results are specified in annexes 3 and 4.

The figures in annex 3 show the cross-sections before and after the fire exposure and the true location of the measuring points, measured after the tests. As an example the results for the specimens GL 26a and GL 82a are shown in figure 4.4.1.

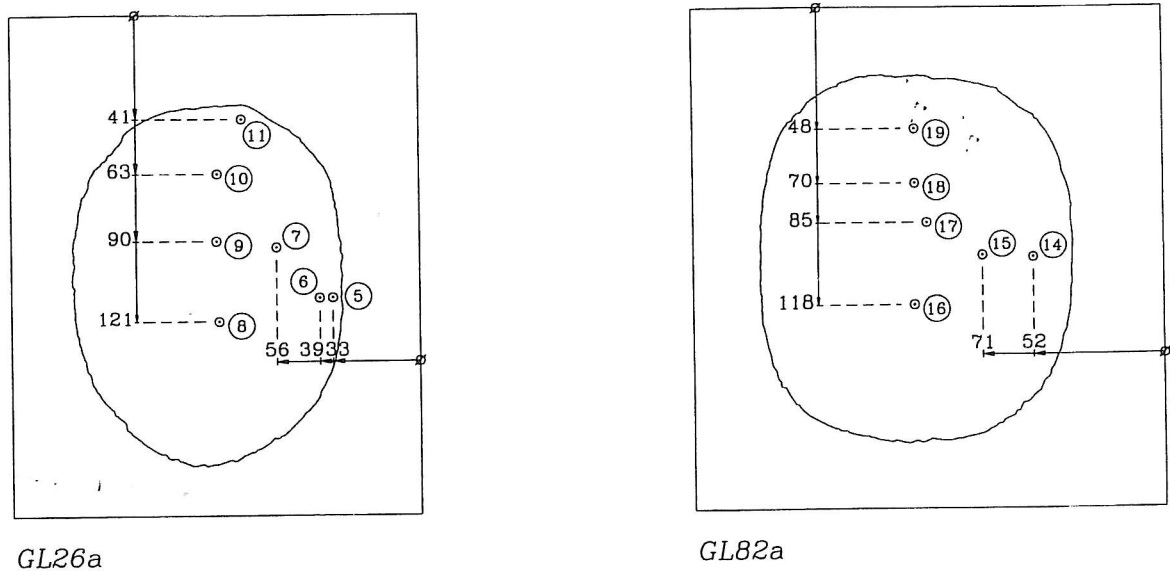


Figure 4.4.1 True location of measuring points in GL 26a and GL 82a.

Annex 4 deals with the relationship between the thermal fire load, the charring depth and the temperatures inside the specimen illustrated in graphs. As an example the graphs for GL 26a are shown in figure 4.4.2.

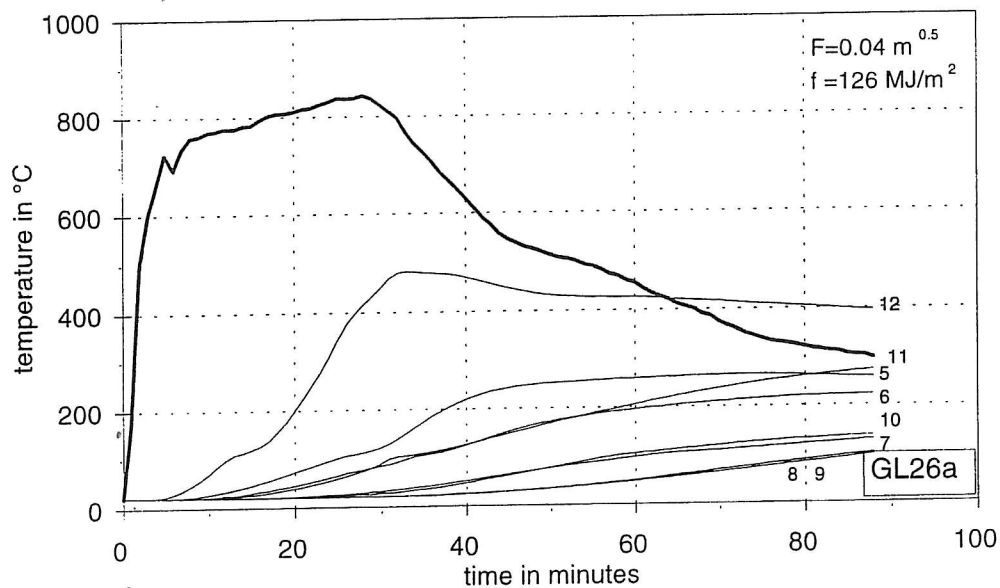
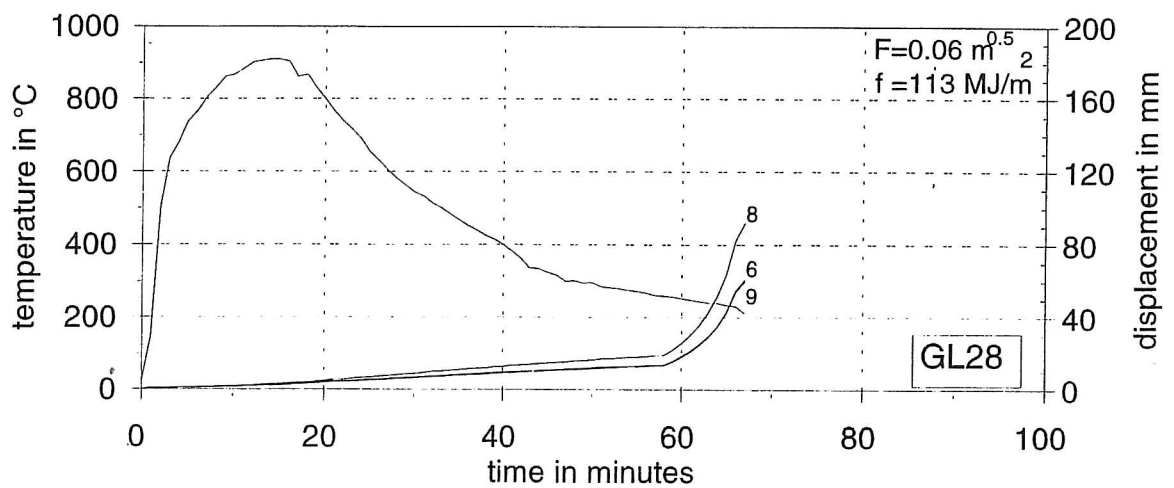
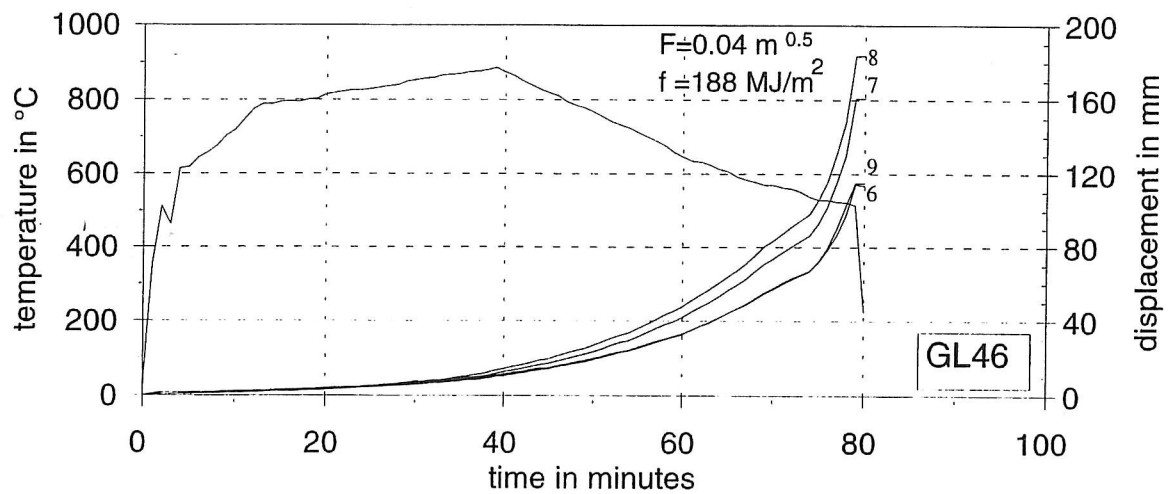
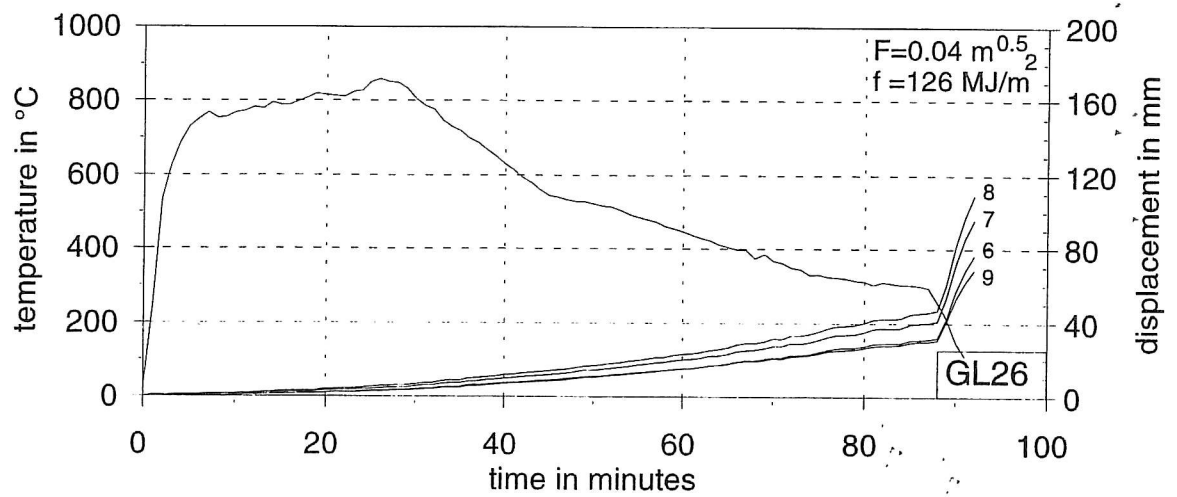
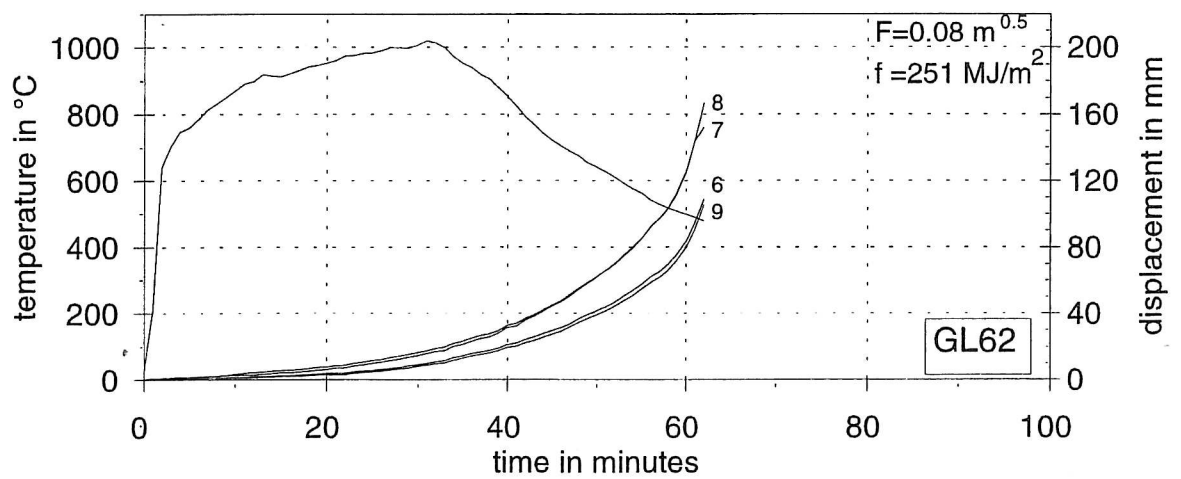
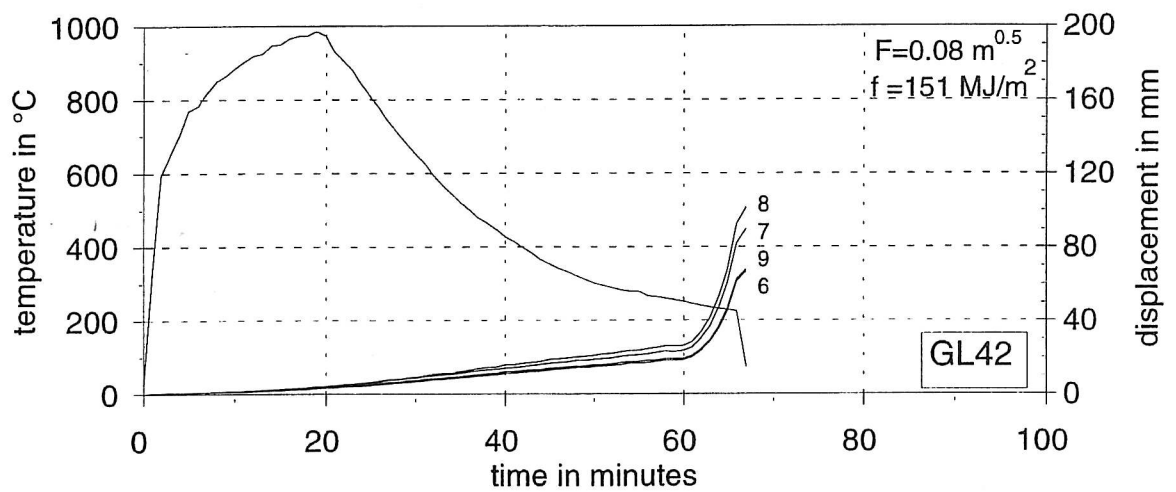
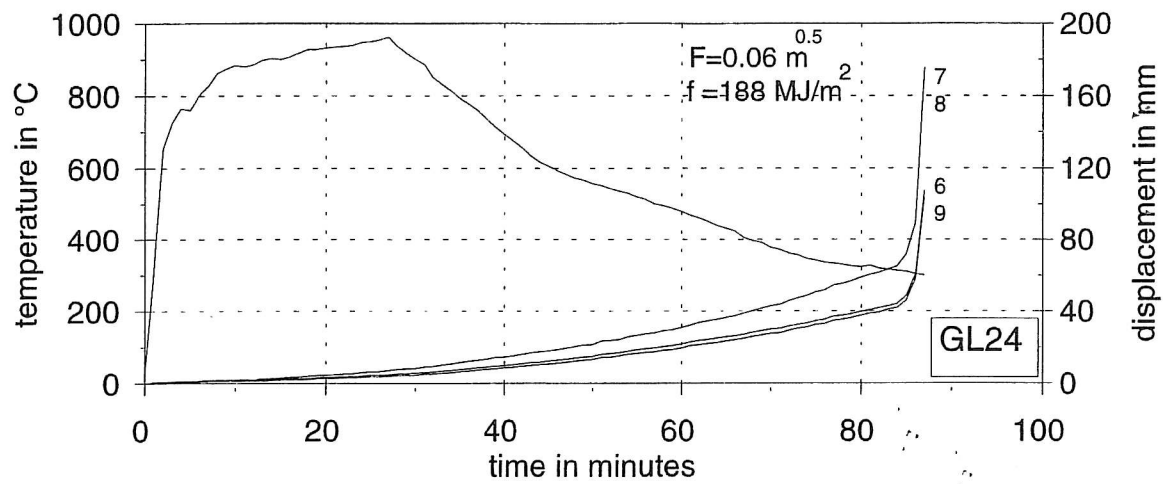


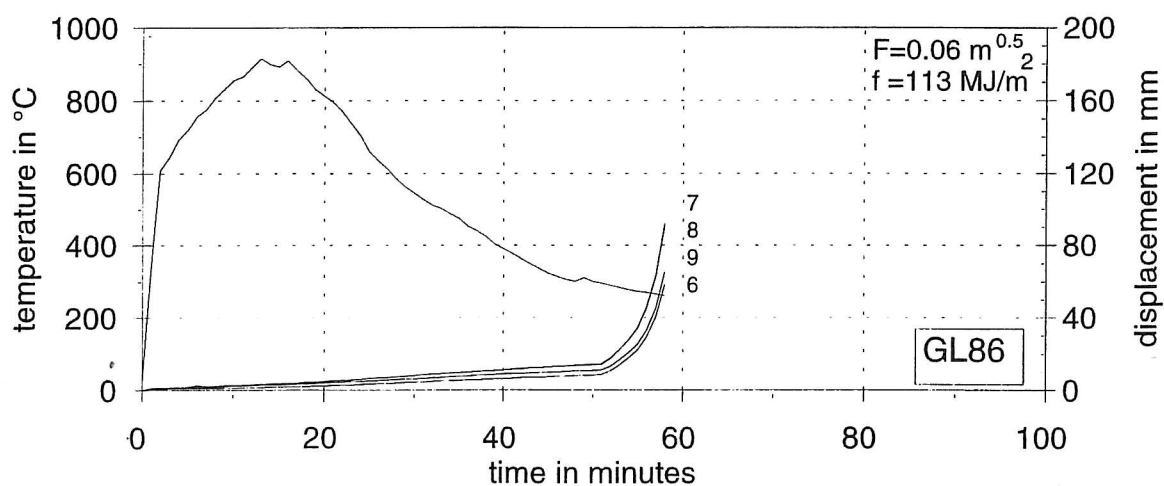
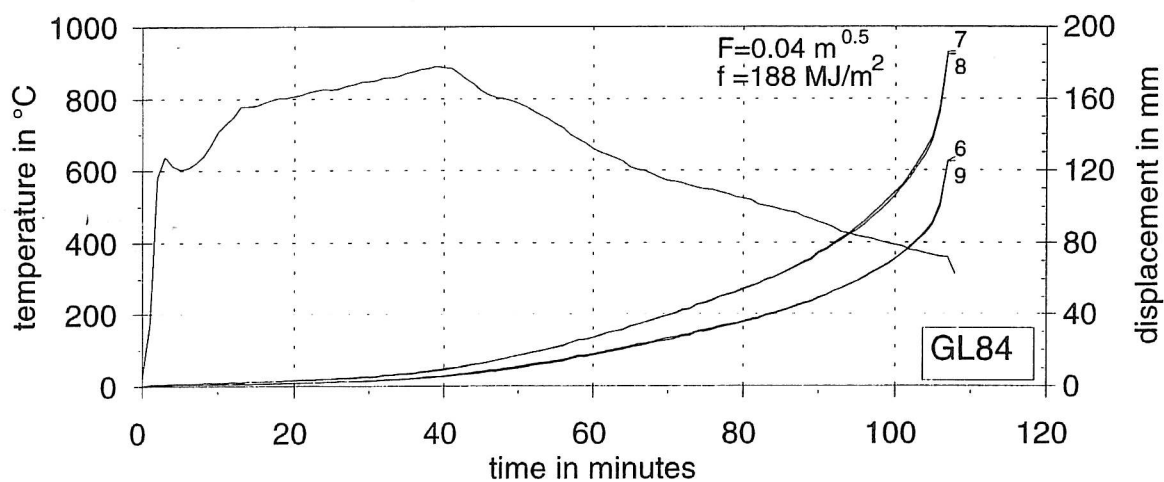
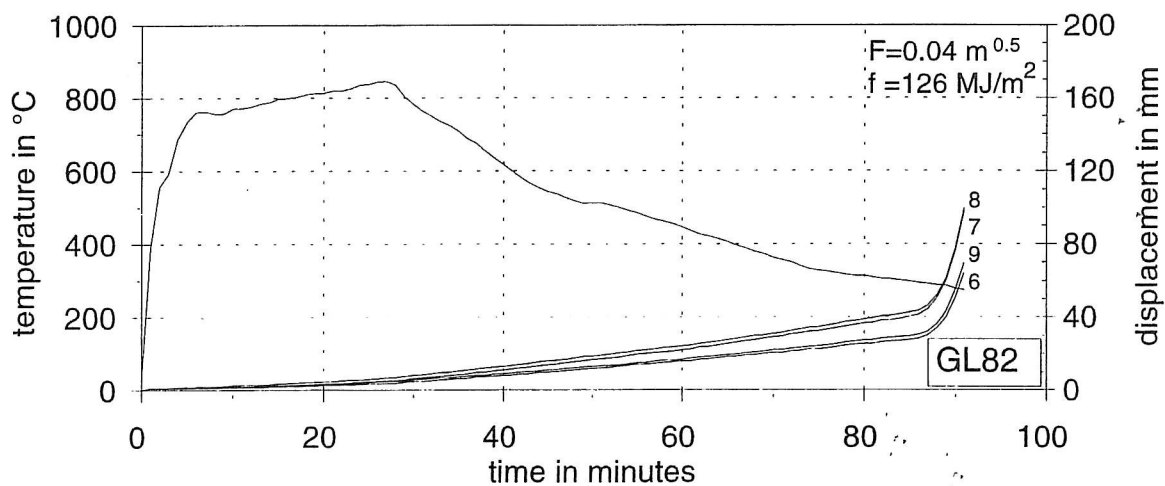
Figure 4.4.2 Temperature graphs for GL 26a.



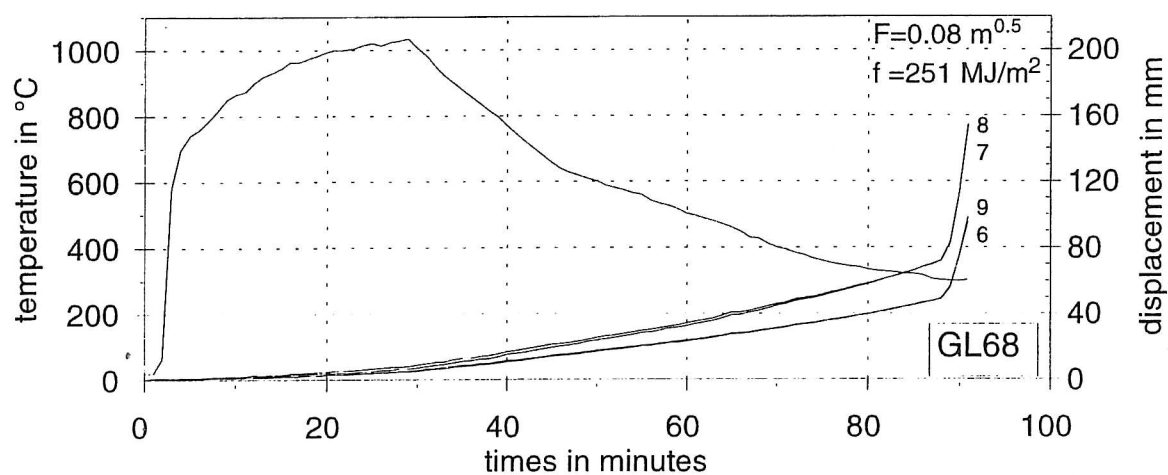
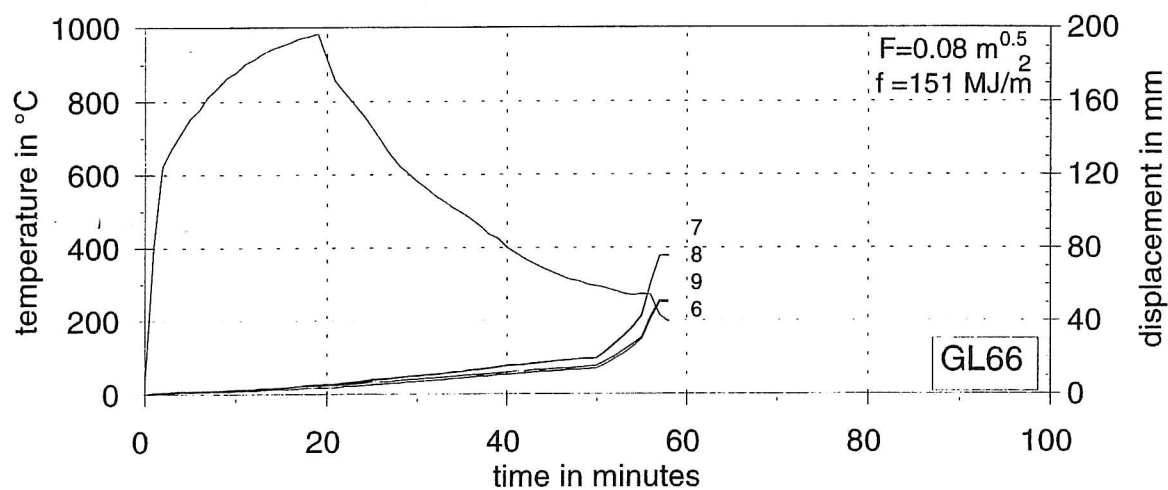
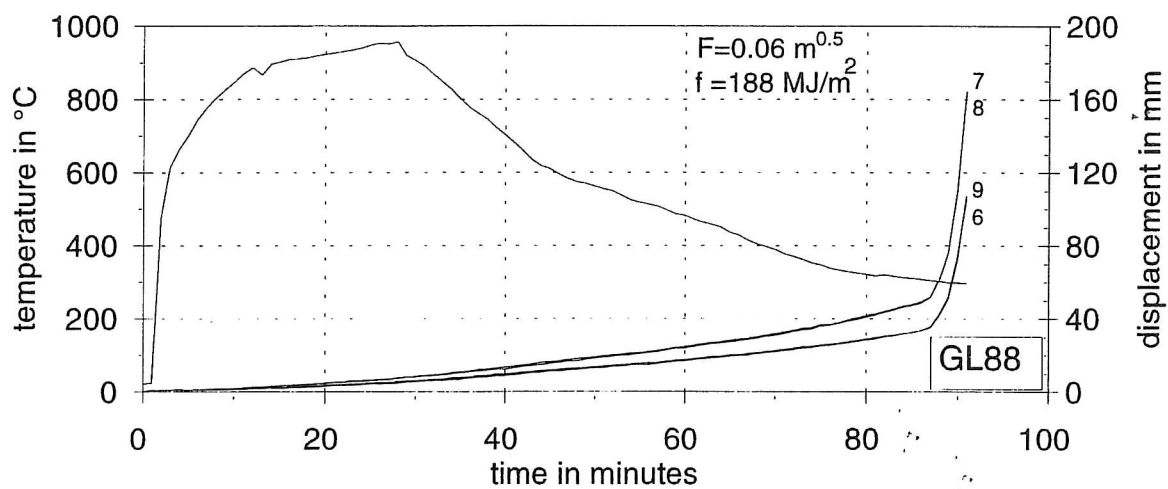
Thermal fire load and displacements at the points 6, 7, 8, and 9.



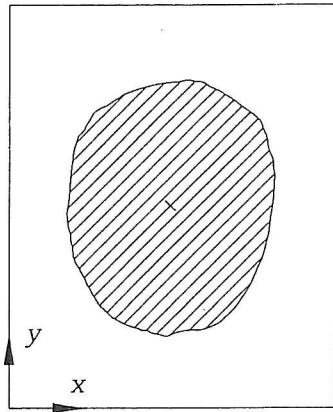
Thermal fire load and displacements at the points 6, 7, 8, and 9.



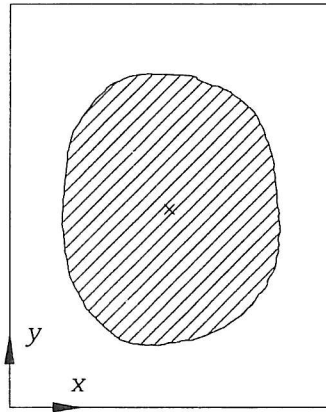
Thermal fire load and displacements at the points 6, 7, 8, and 9.



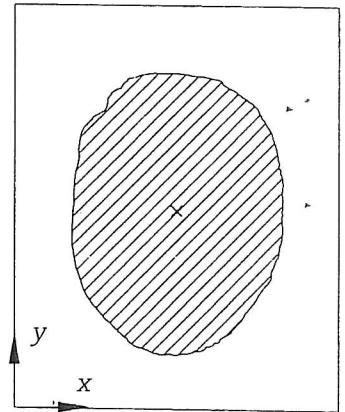
Thermal fire load and displacements at the points 6, 7, 8, and 9.



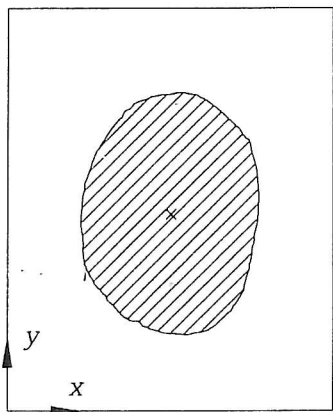
GL26A



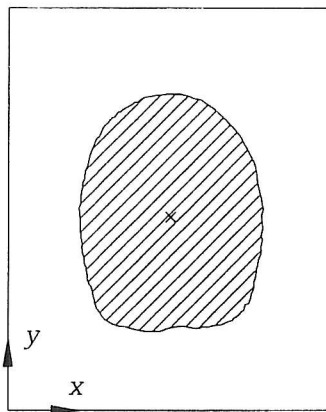
GL26B+20



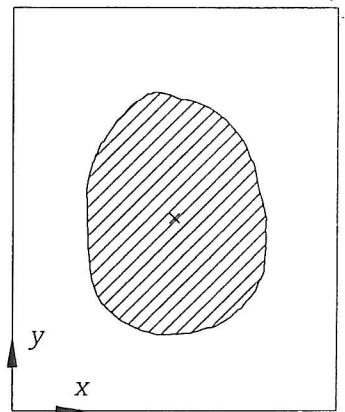
GL26C



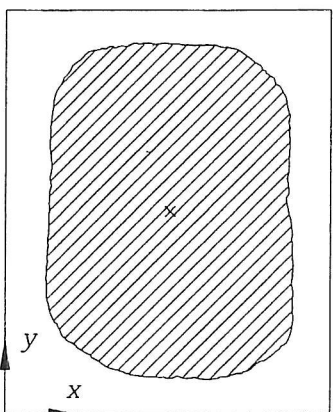
GL46A



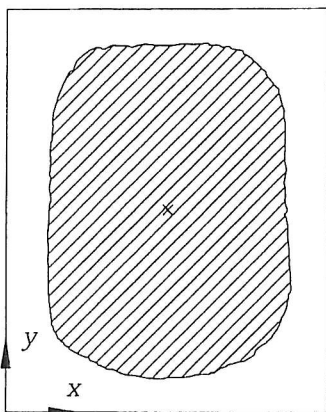
GL46B



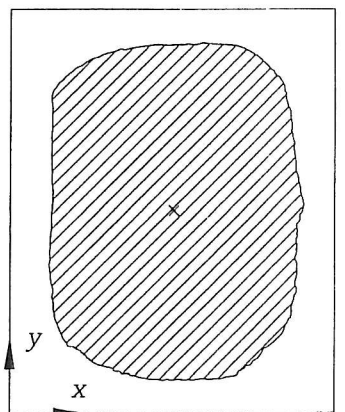
GL46C



GL28A

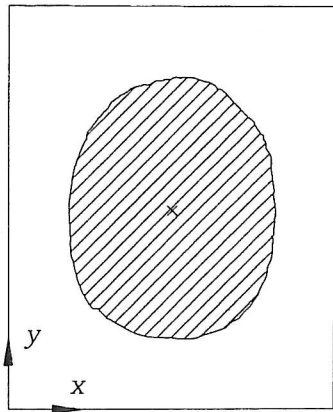


GL28B+20

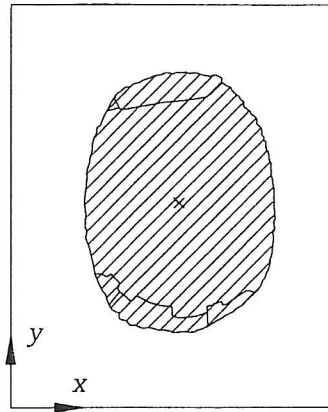


GL28C

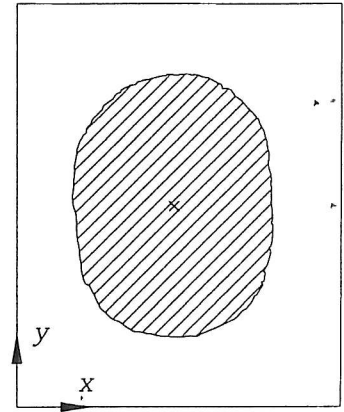
Cross-section A, B and C, before and after fire exposure.



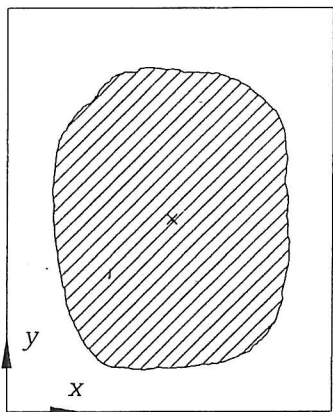
GL24A



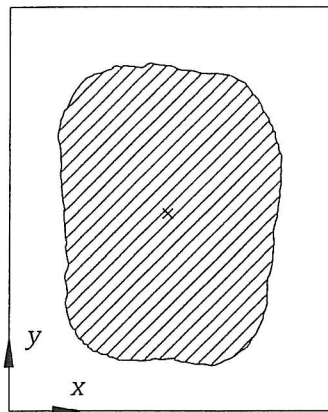
GL24B



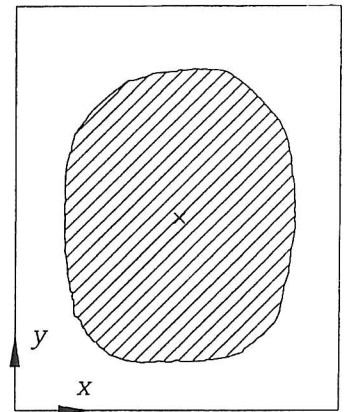
GL24C



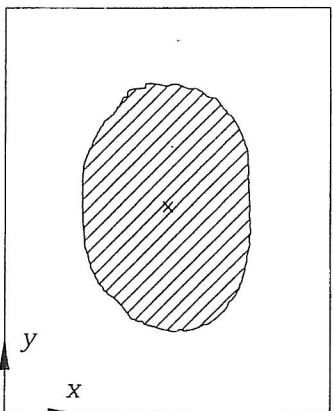
GL42A



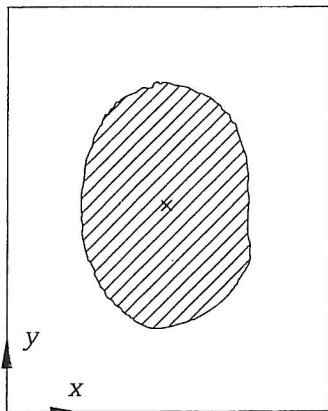
GL42B+20mm



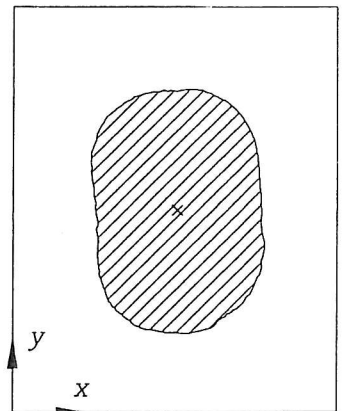
GL42C



GL62A

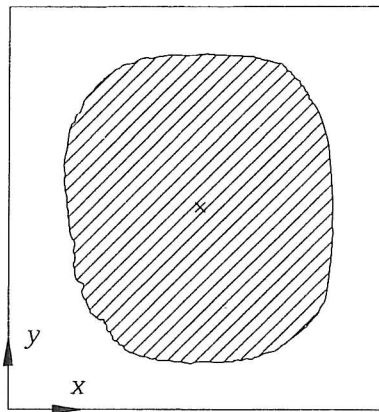


GL62B

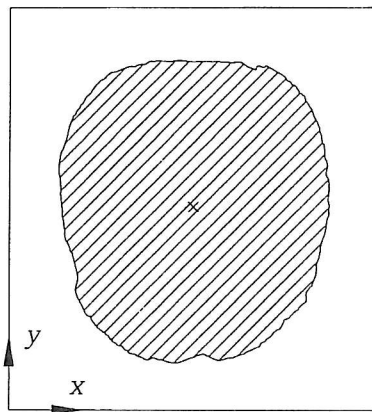


GL62C

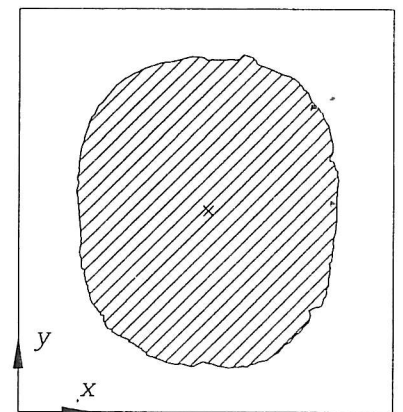
Cross-section A, B and C, before and after fire exposure.



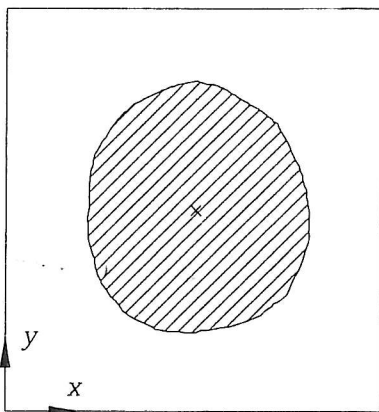
GL82A



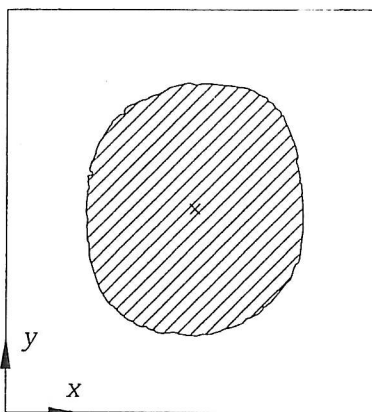
GL82B



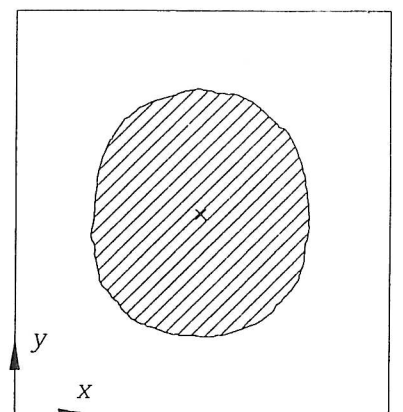
GL82C



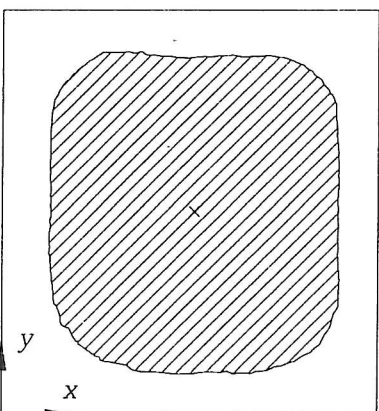
GL84A



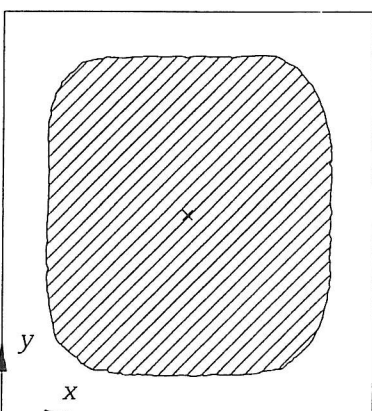
GL84B



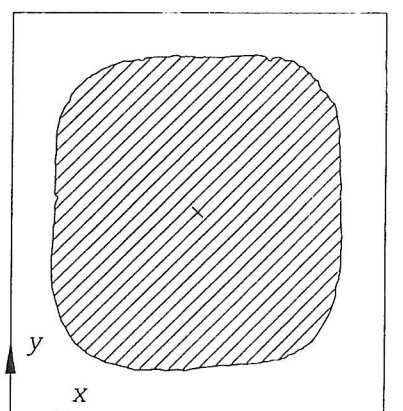
GL84C



GL86A

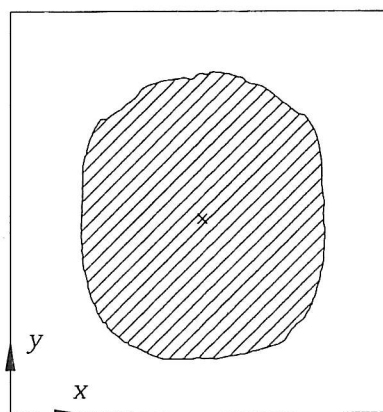


GL86B

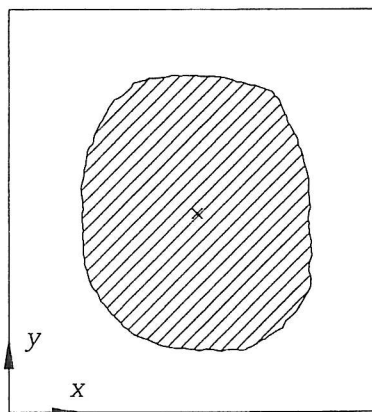


GL86C

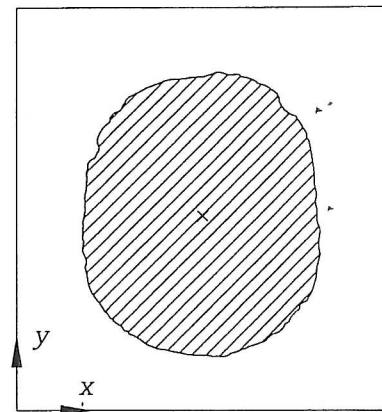
Cross-section A, B and C, before and after fire exposure.



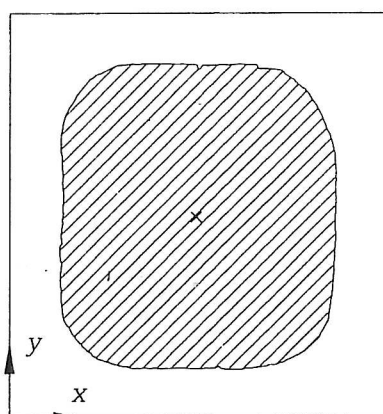
GL88A



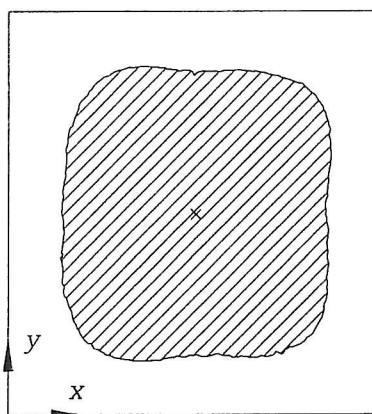
GL88B



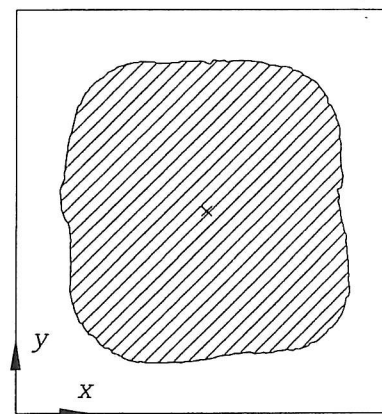
GL88C



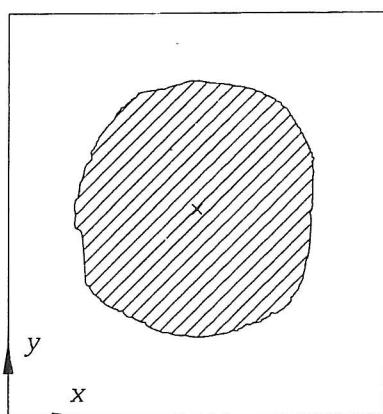
GL66A



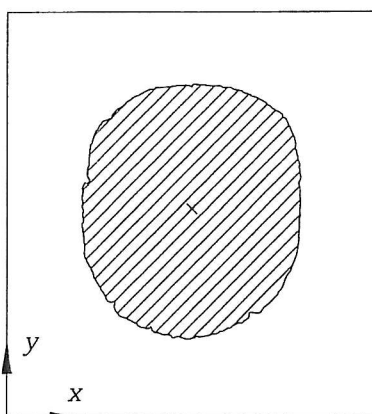
GL66B



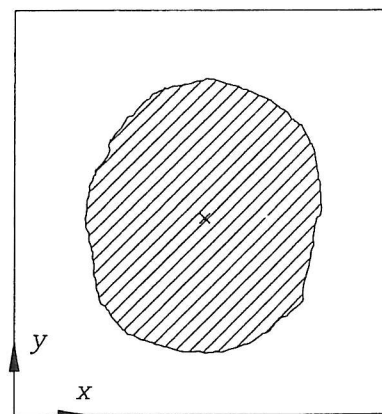
GL66C



GL68A



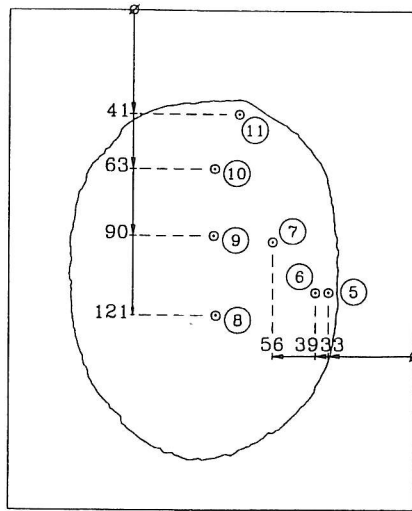
GL68B



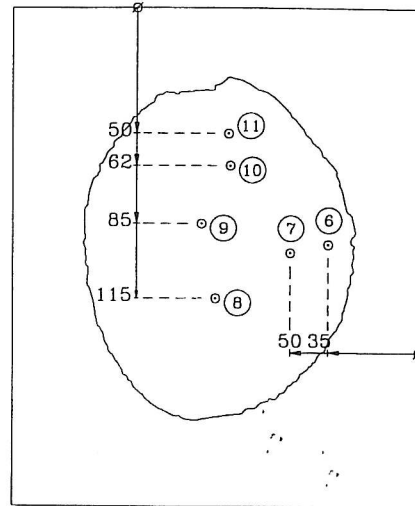
GL68C

Cross-section A, B and C, before and after fire exposure.

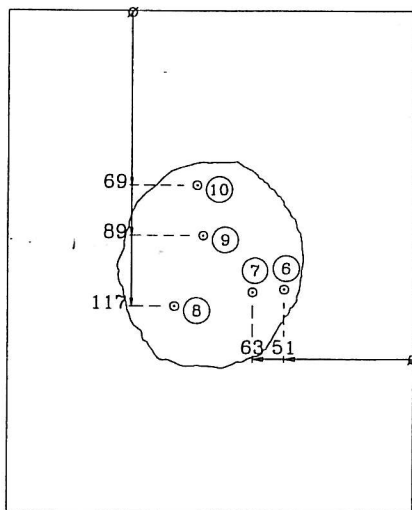
Annex 3.1



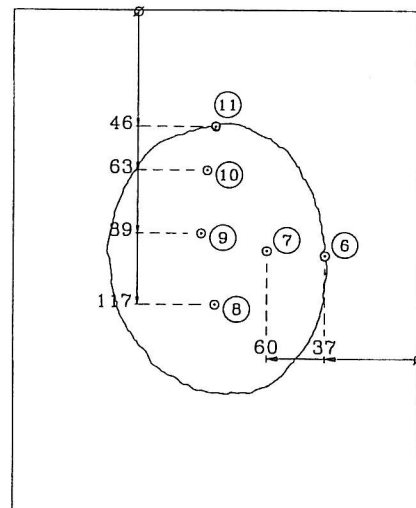
GL26a



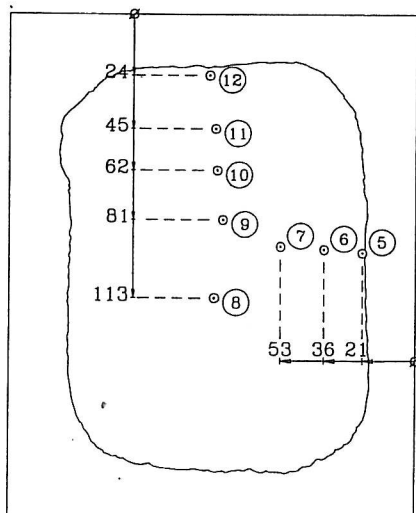
GL26b



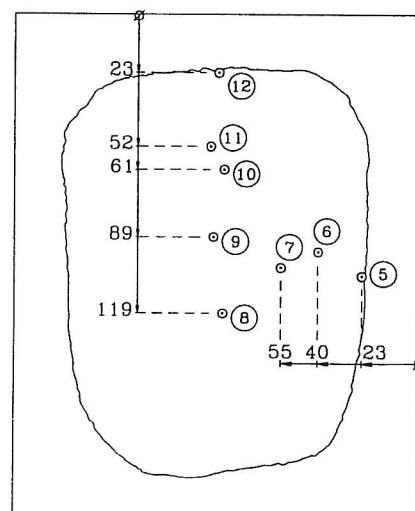
GL46a



GL46b

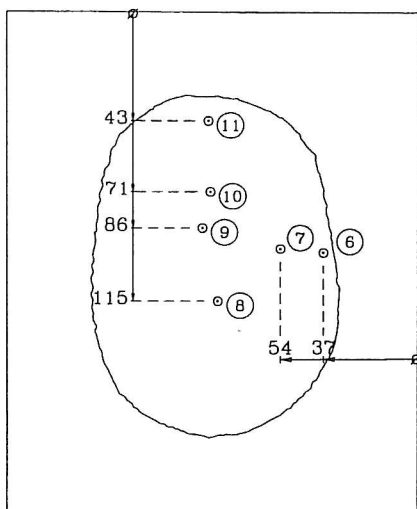


GL28a

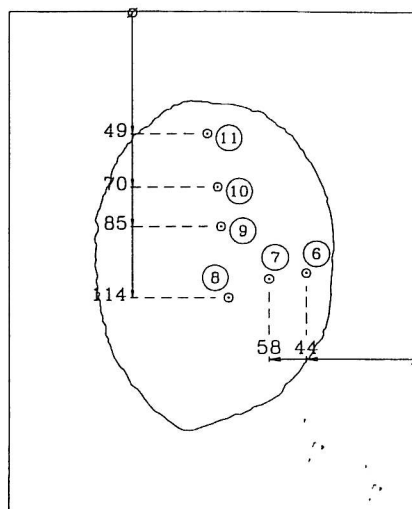


GL28b

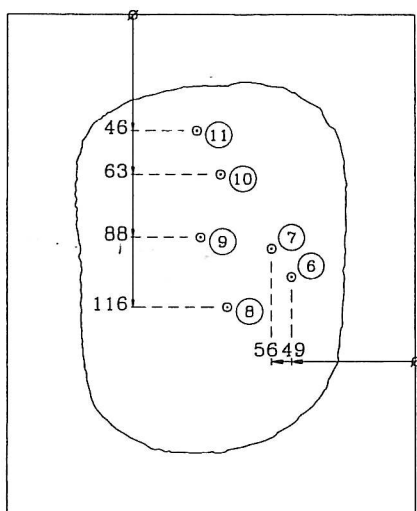
True location of measuring points.



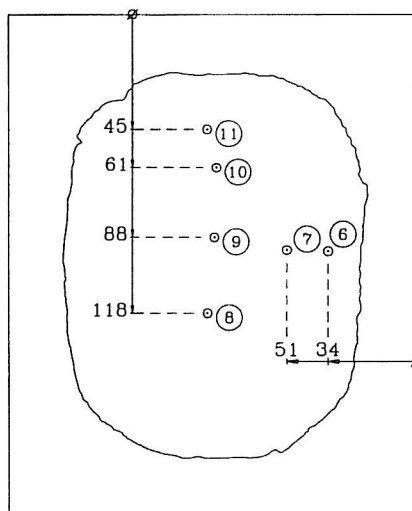
GL24a



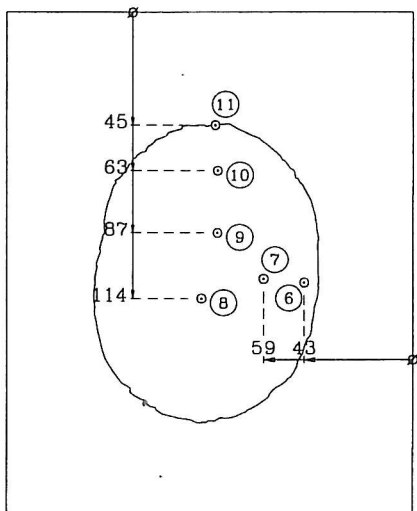
GL24b



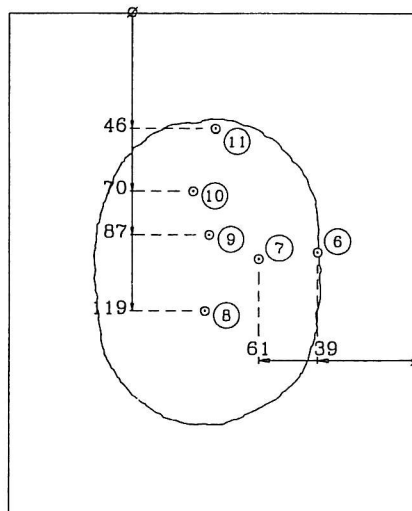
GL42a



GL42b



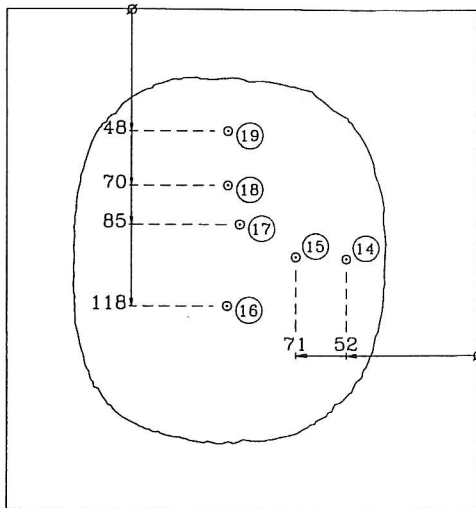
GL62a



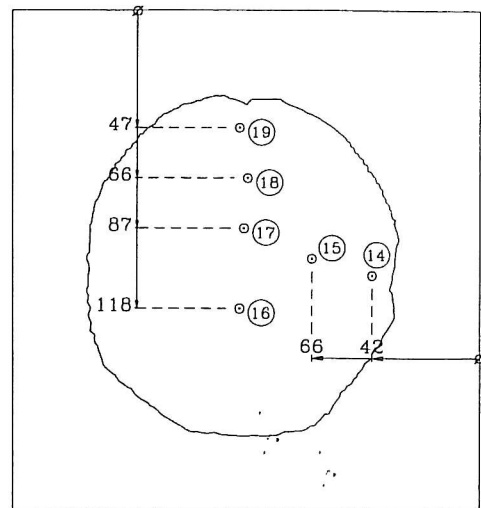
GL62b

True location of measuring points.

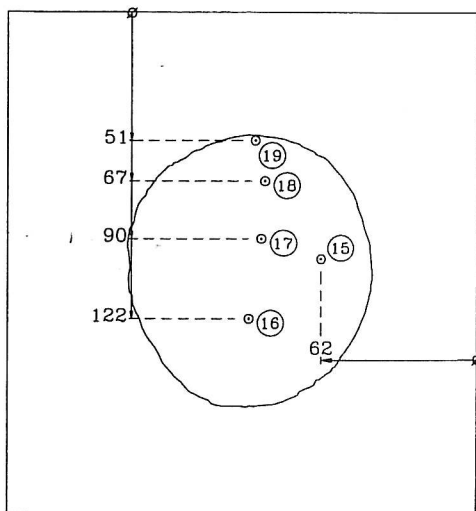
Annex 3.3



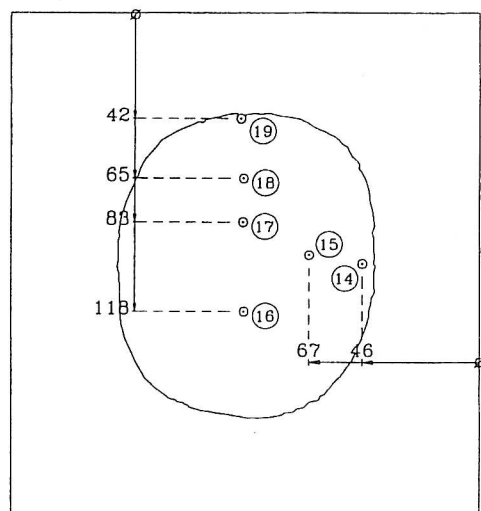
GL82a



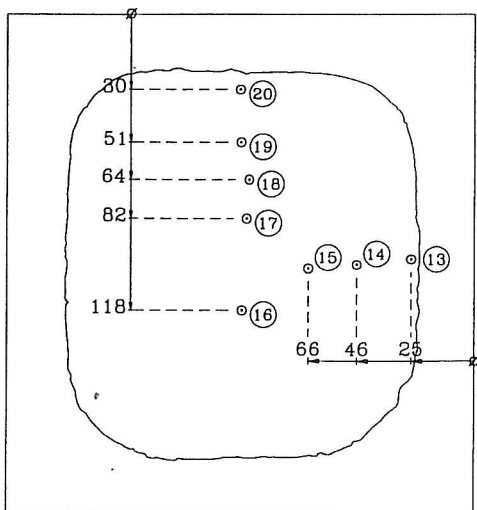
GL82b



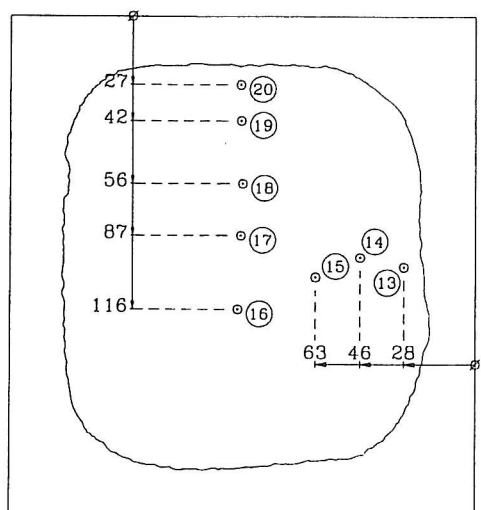
GL84a



GL84b

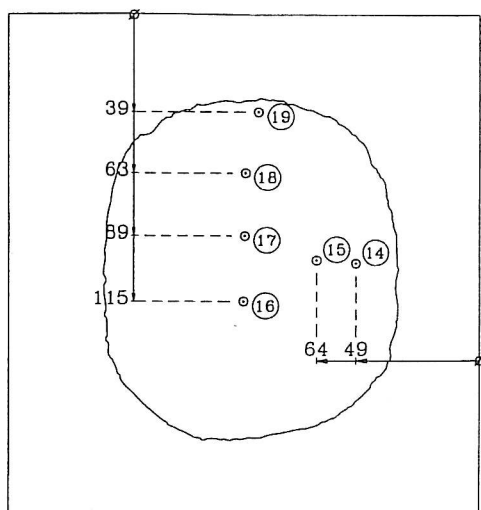


GL86a *

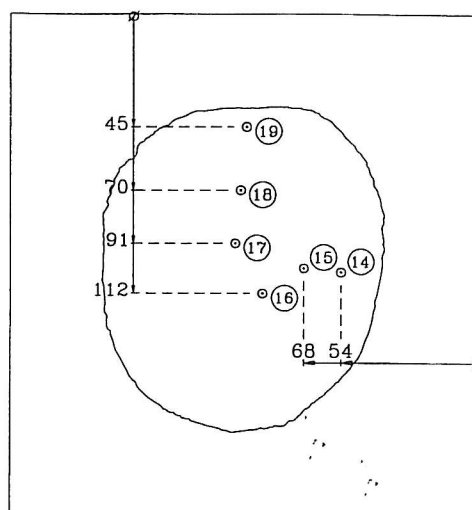


GL86b

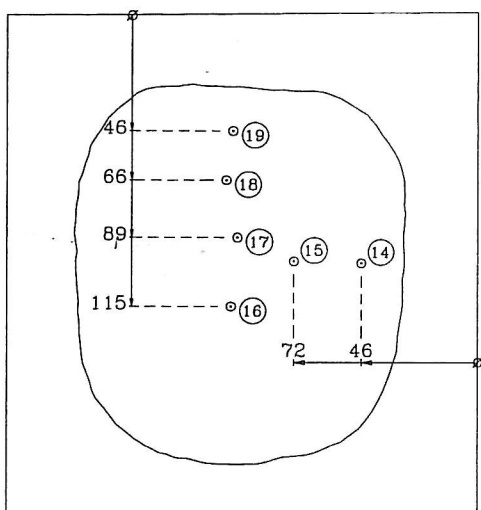
True location of measuring points.



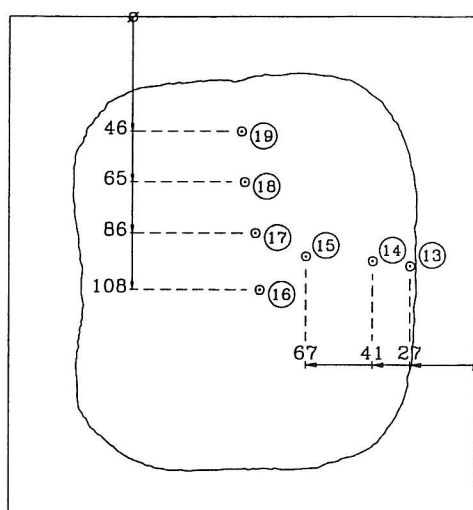
GL88a



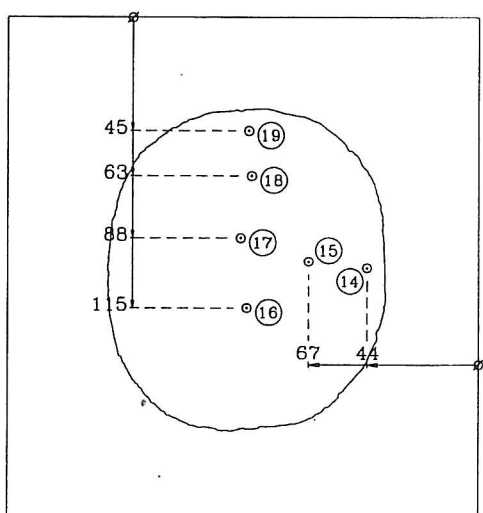
GL88b



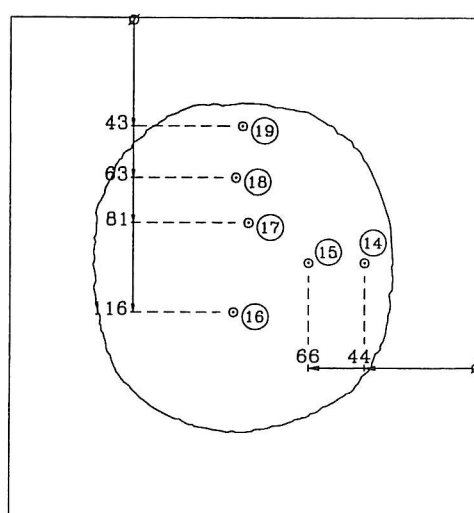
GL66a



GL66b

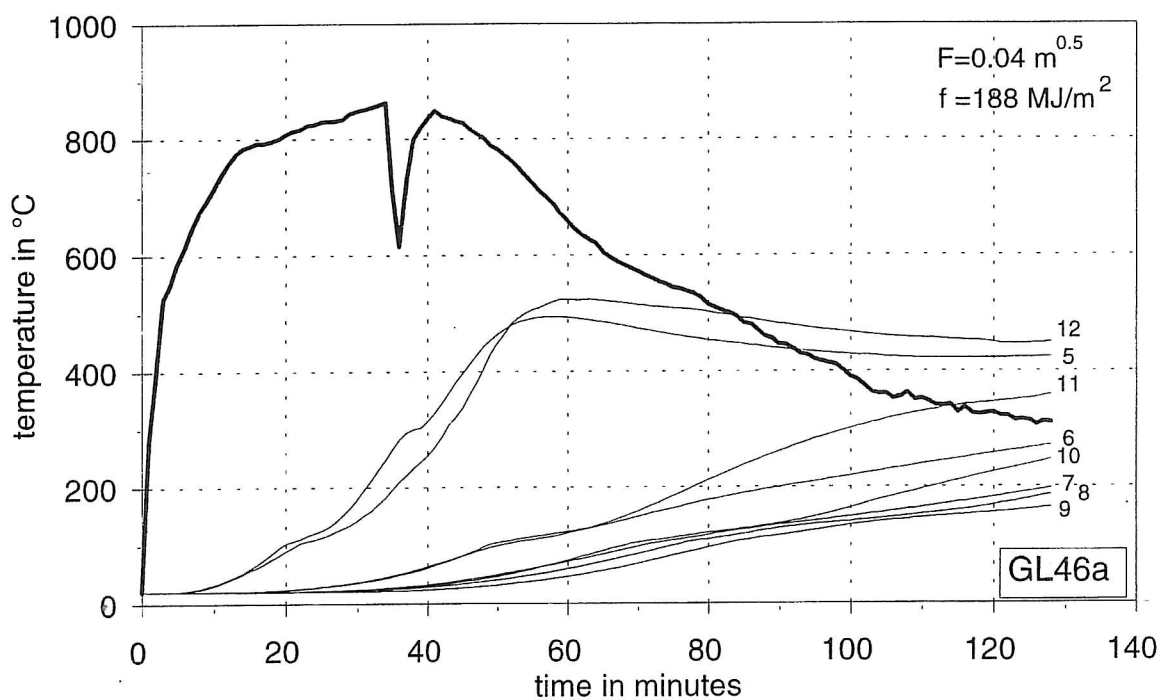
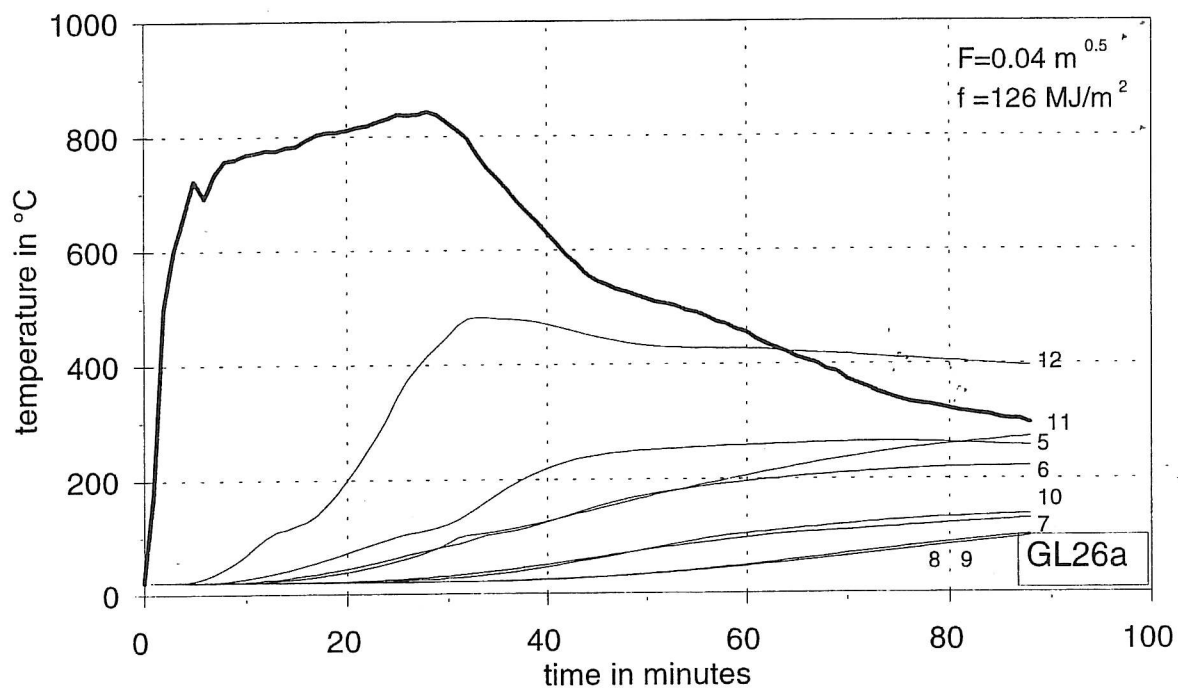


GL68a

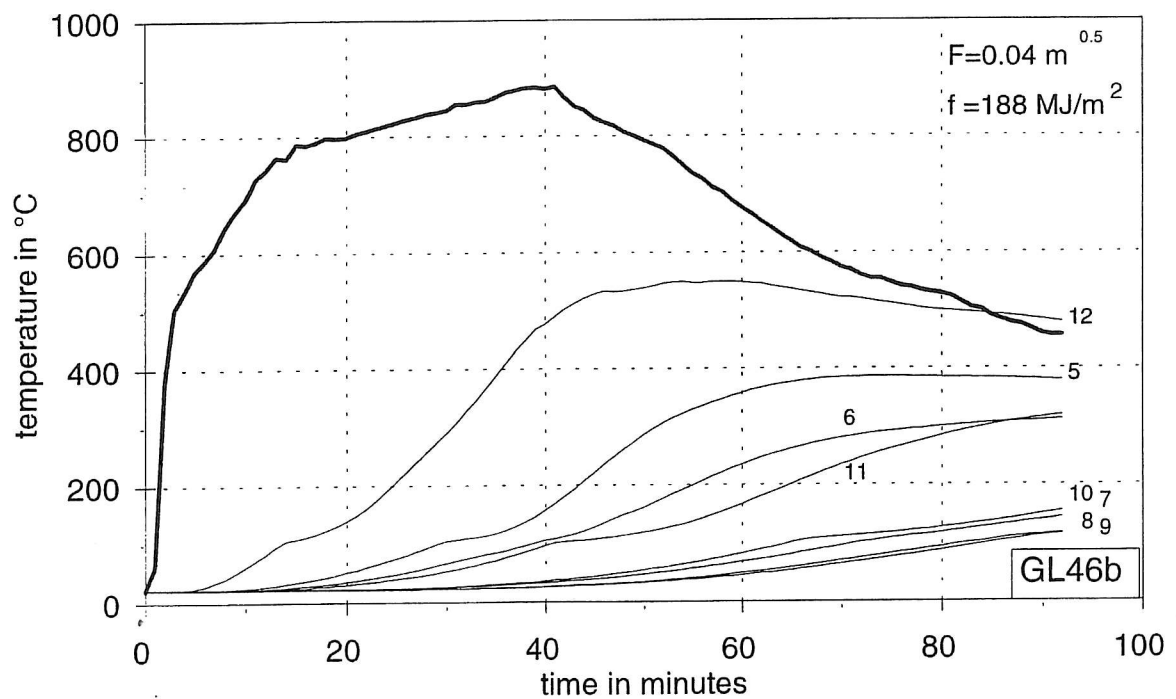
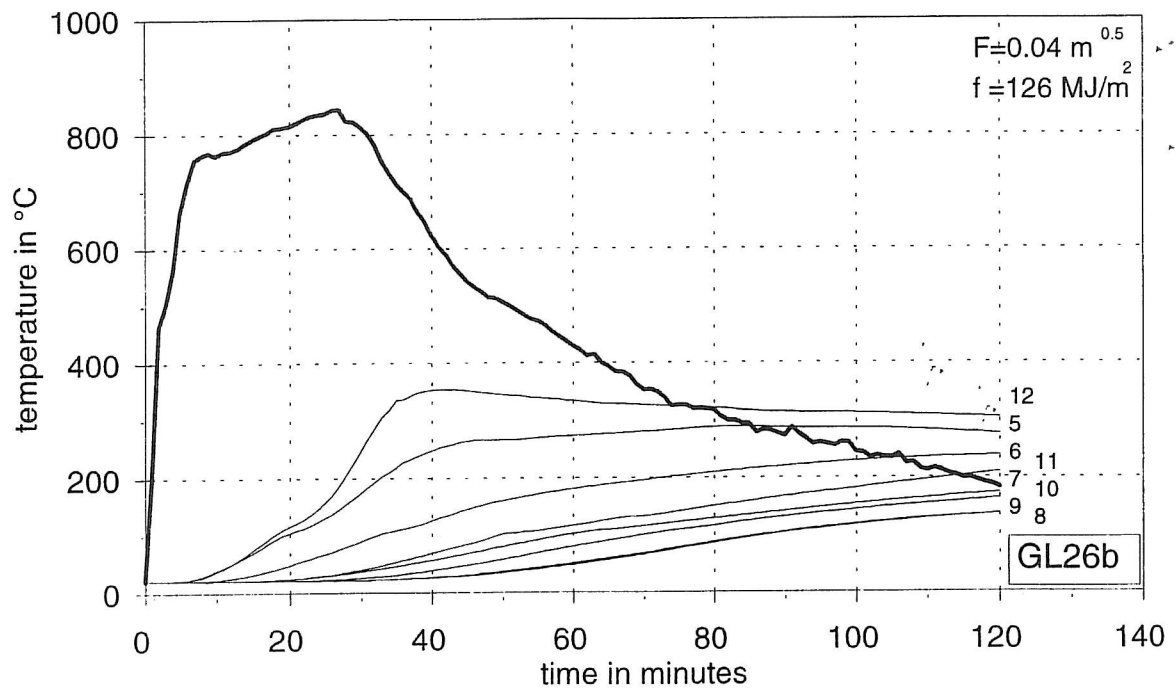


GL68b

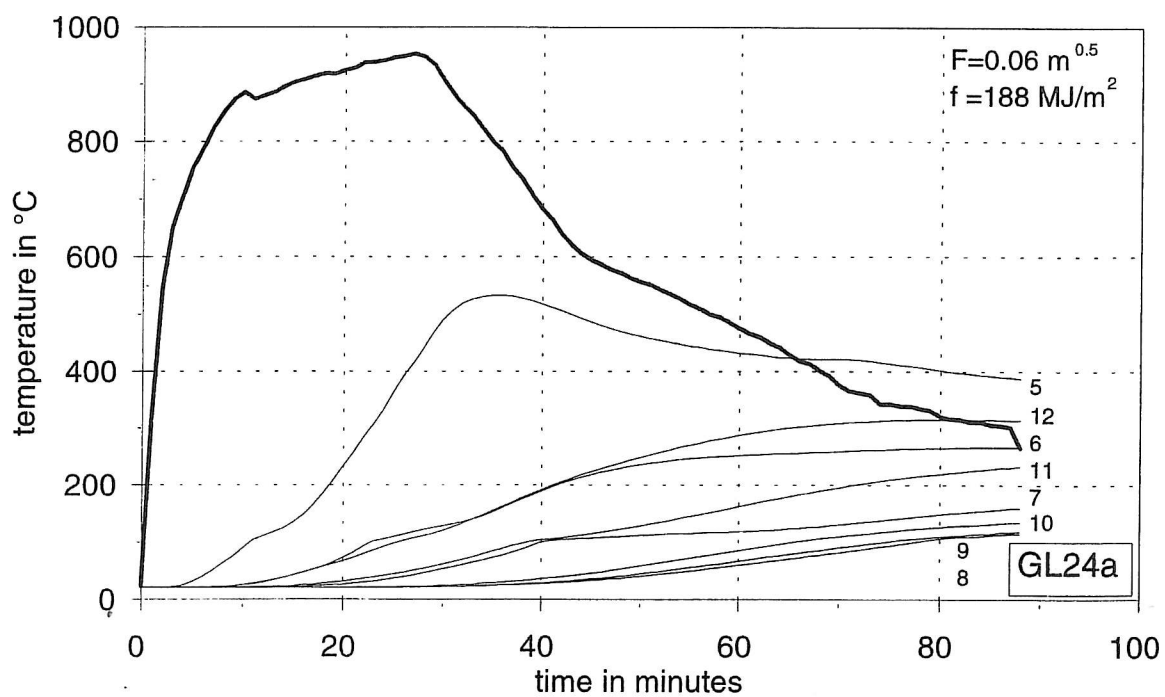
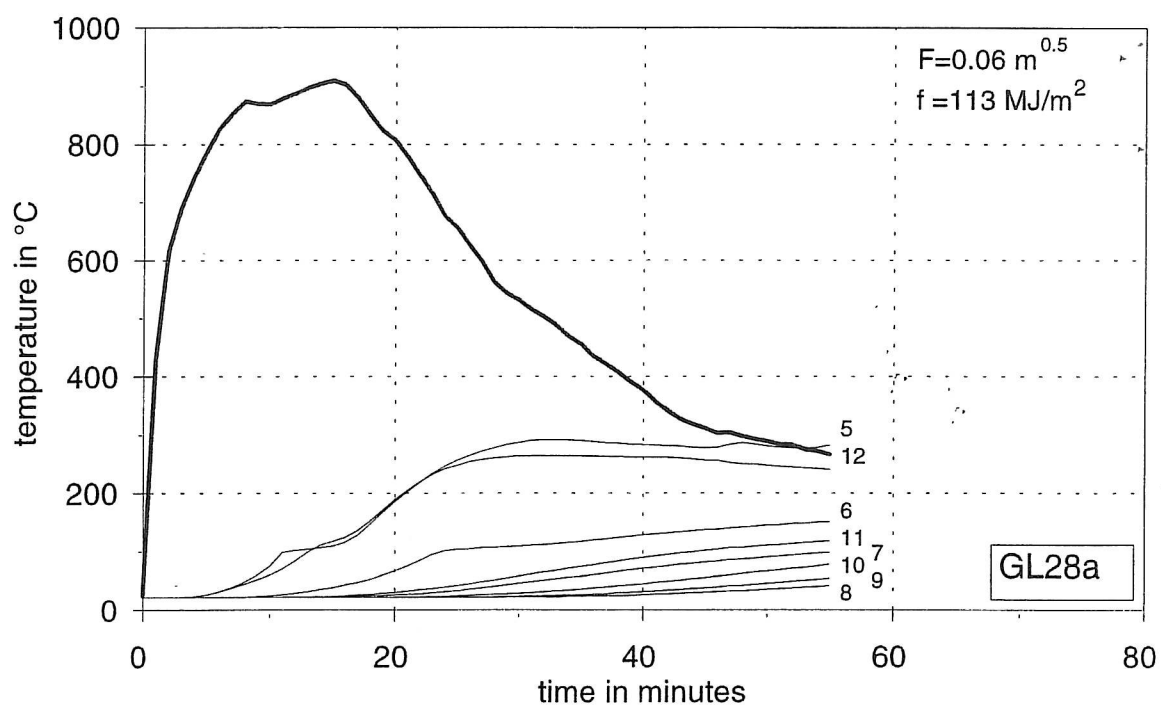
True location of measuring points.



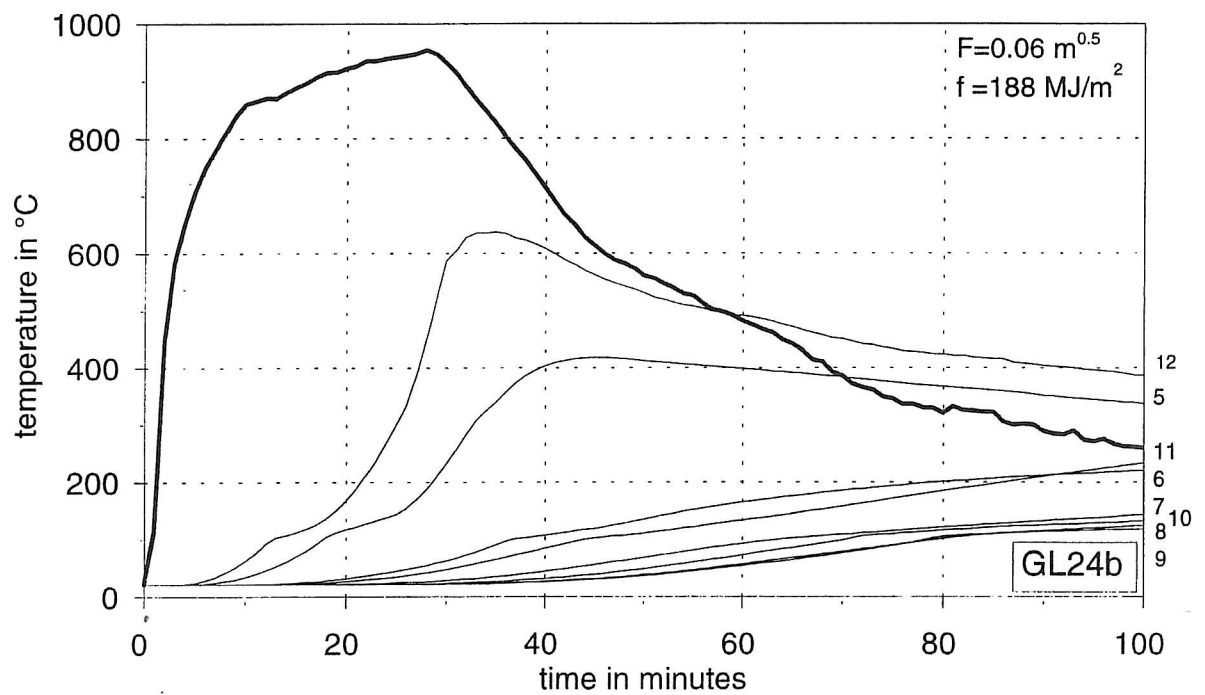
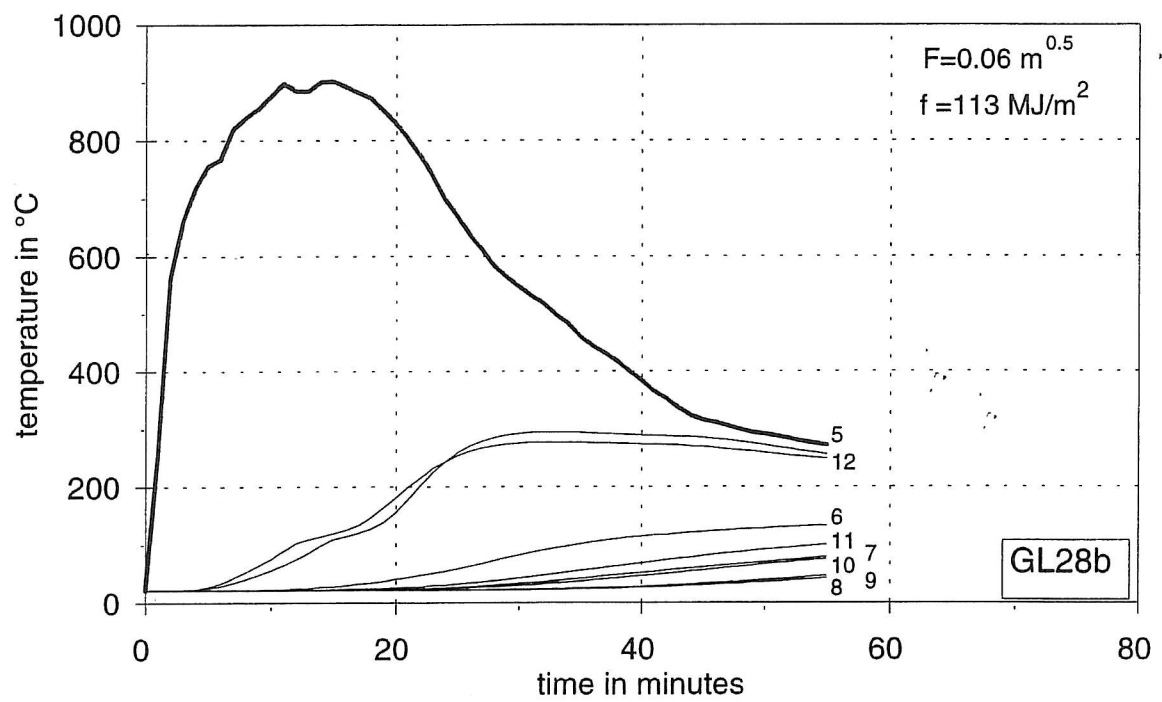
Relationship between fire load, charring depth and temperature inside the beams.



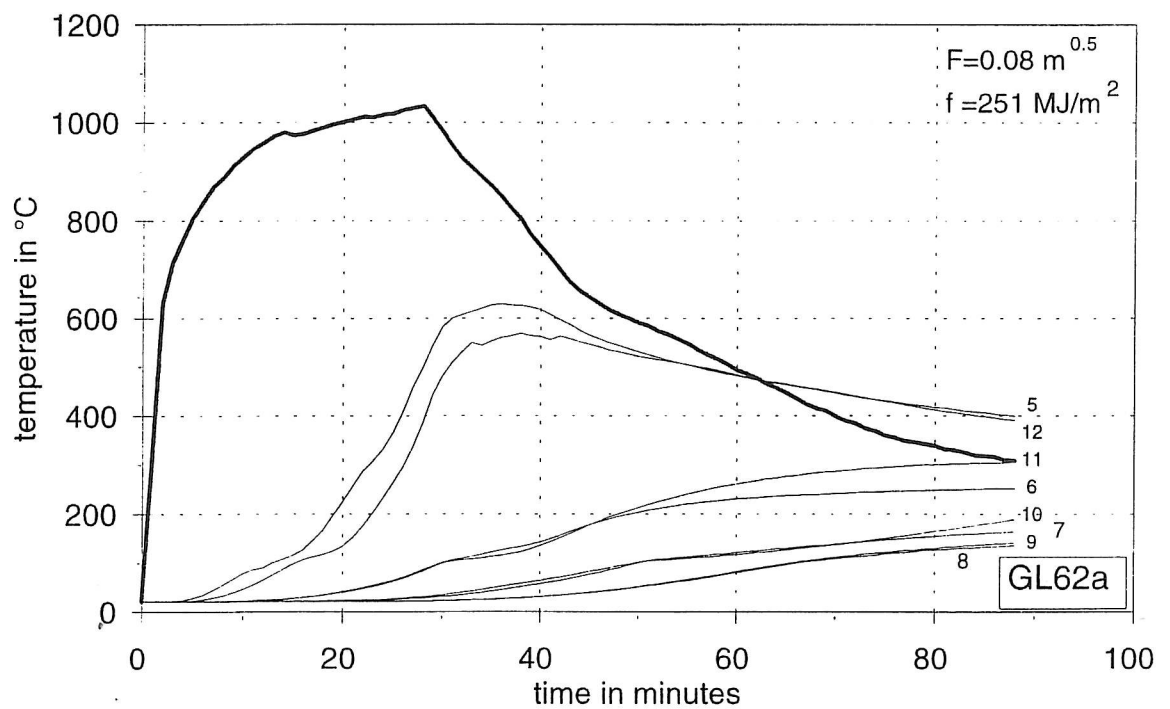
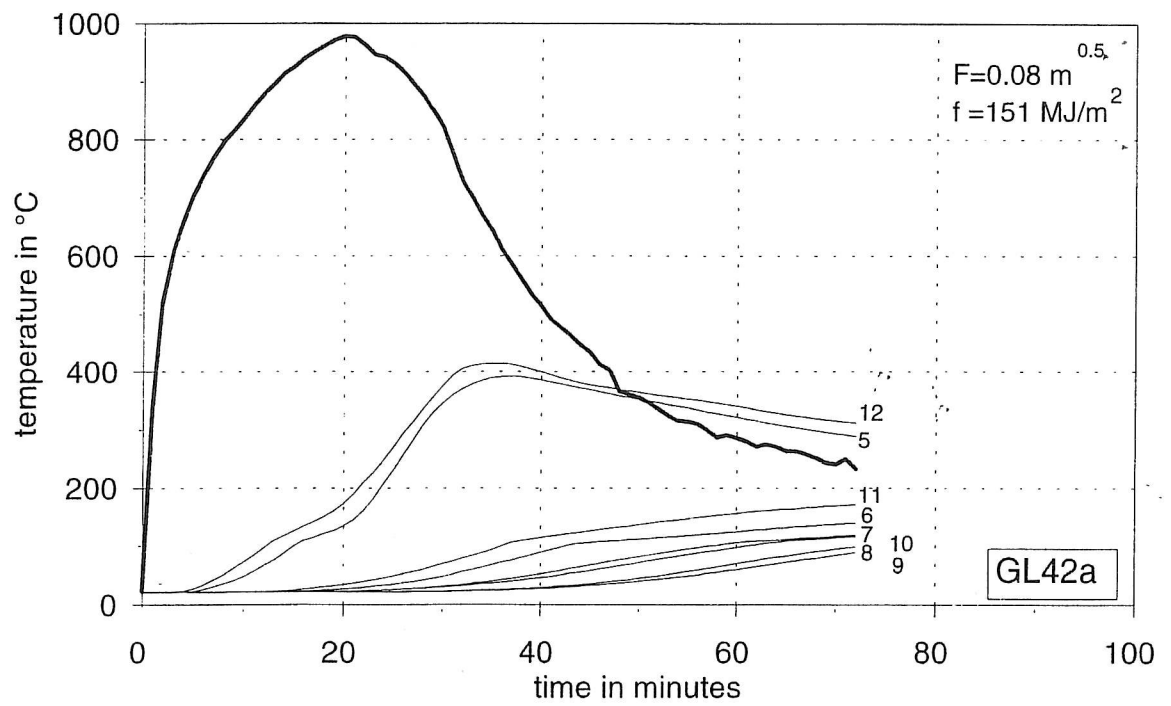
Relationship between fire load, charring depth and temperature inside the beams.



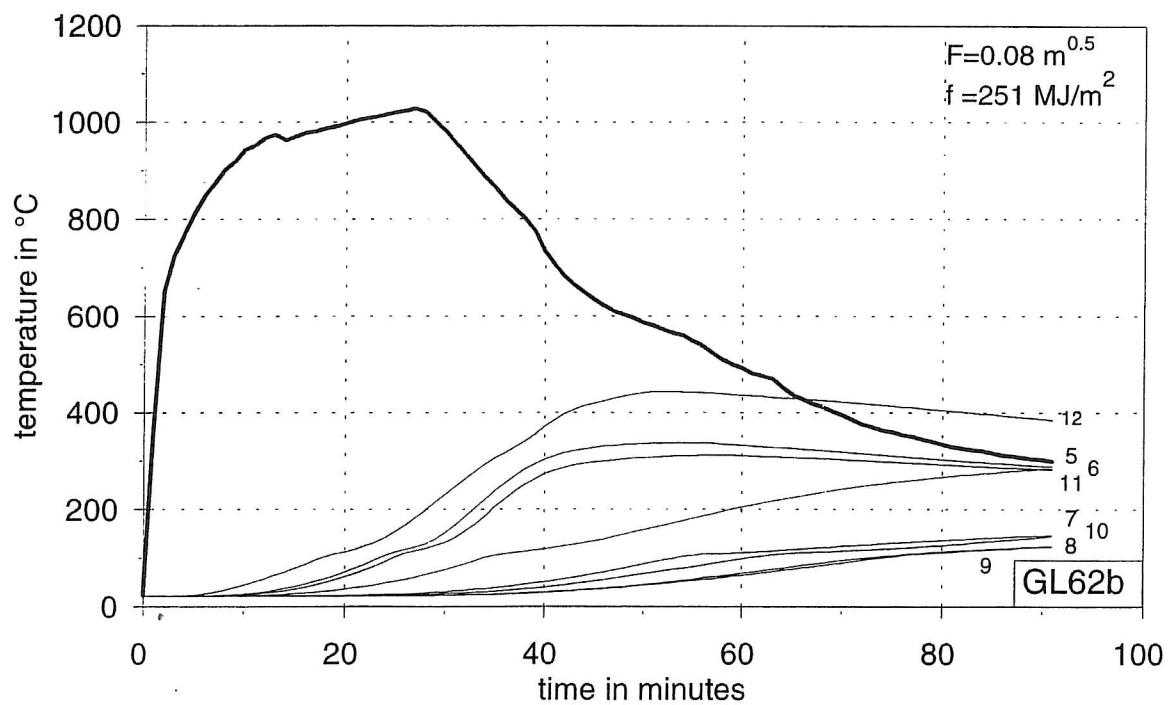
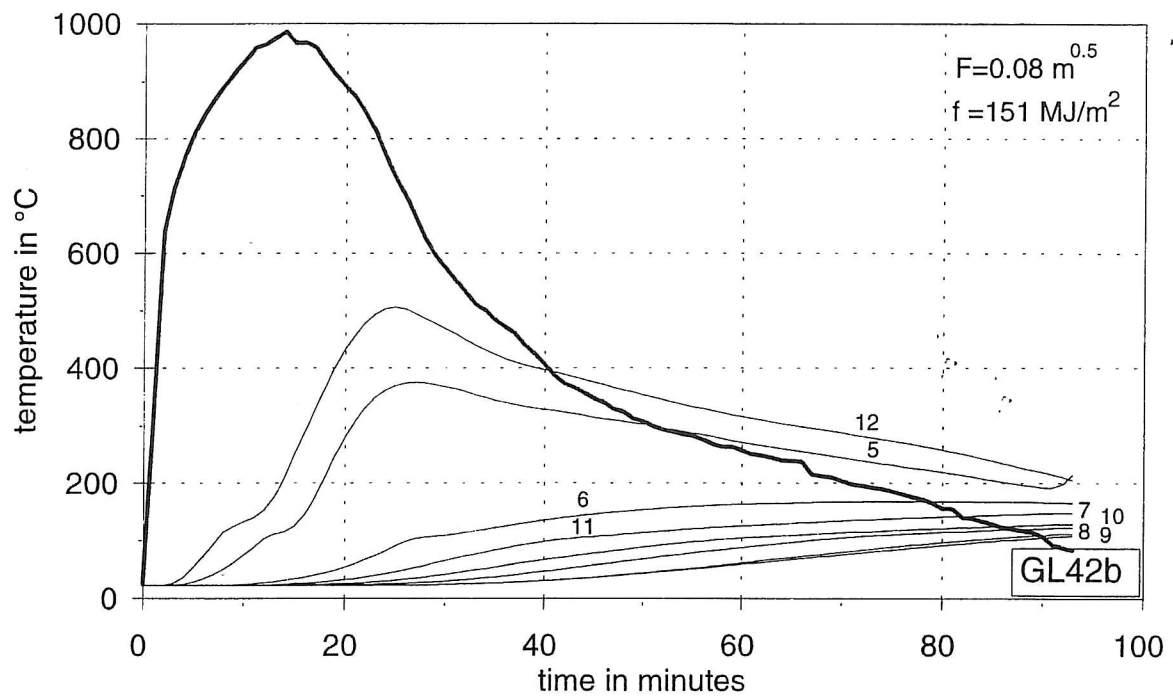
Relationship between fire load, charring depth and temperature inside the beams.



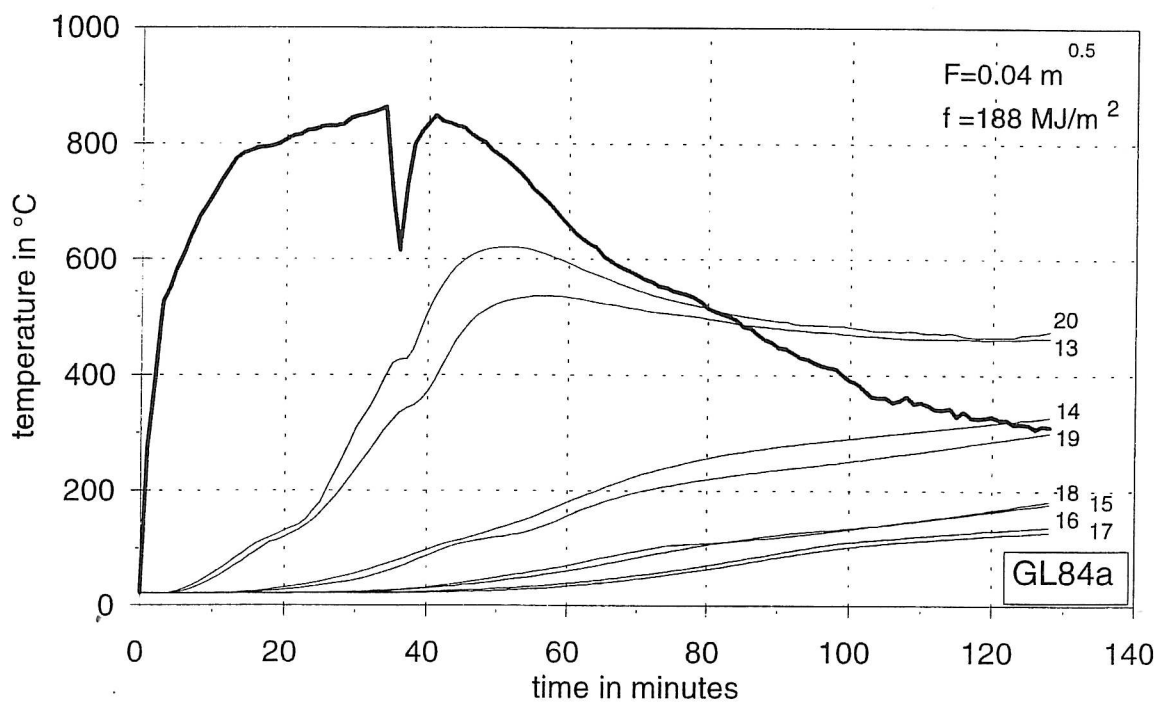
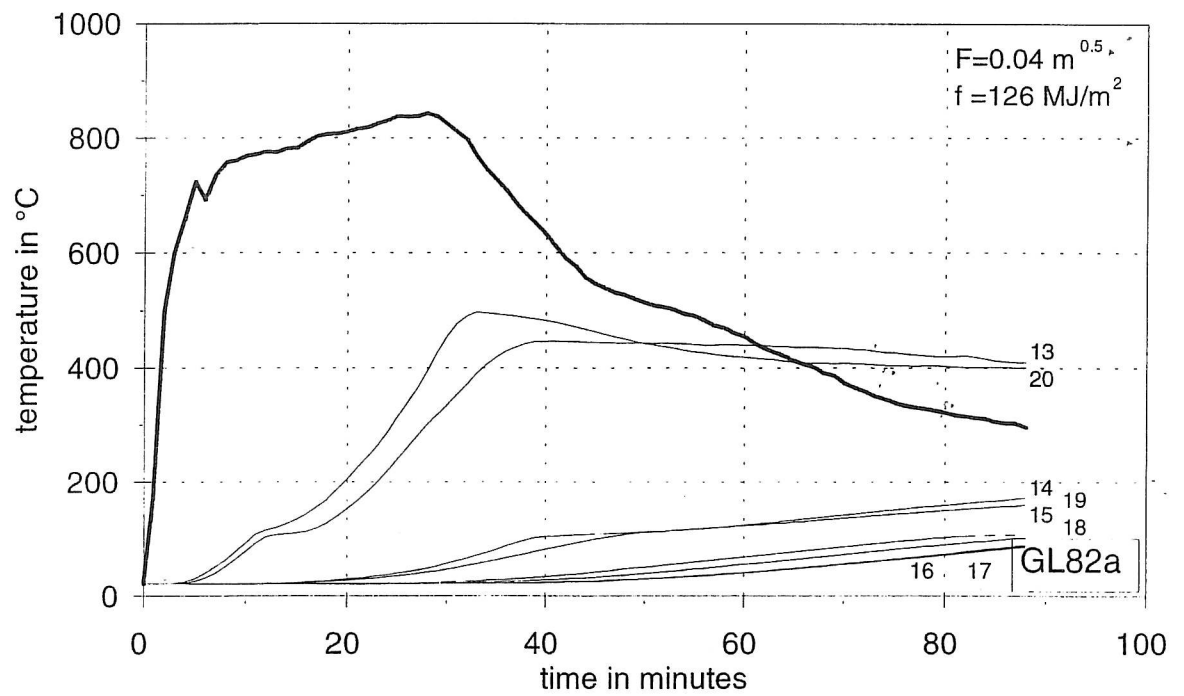
Relationship between fire load, charring depth and temperature inside the beams.



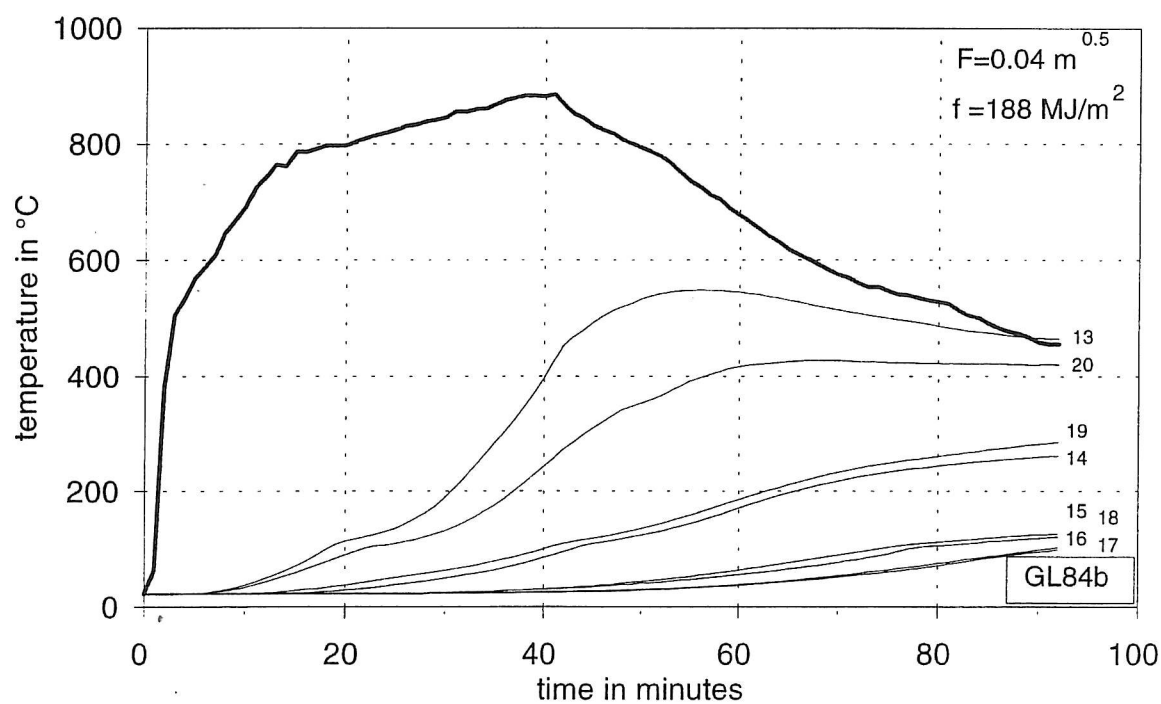
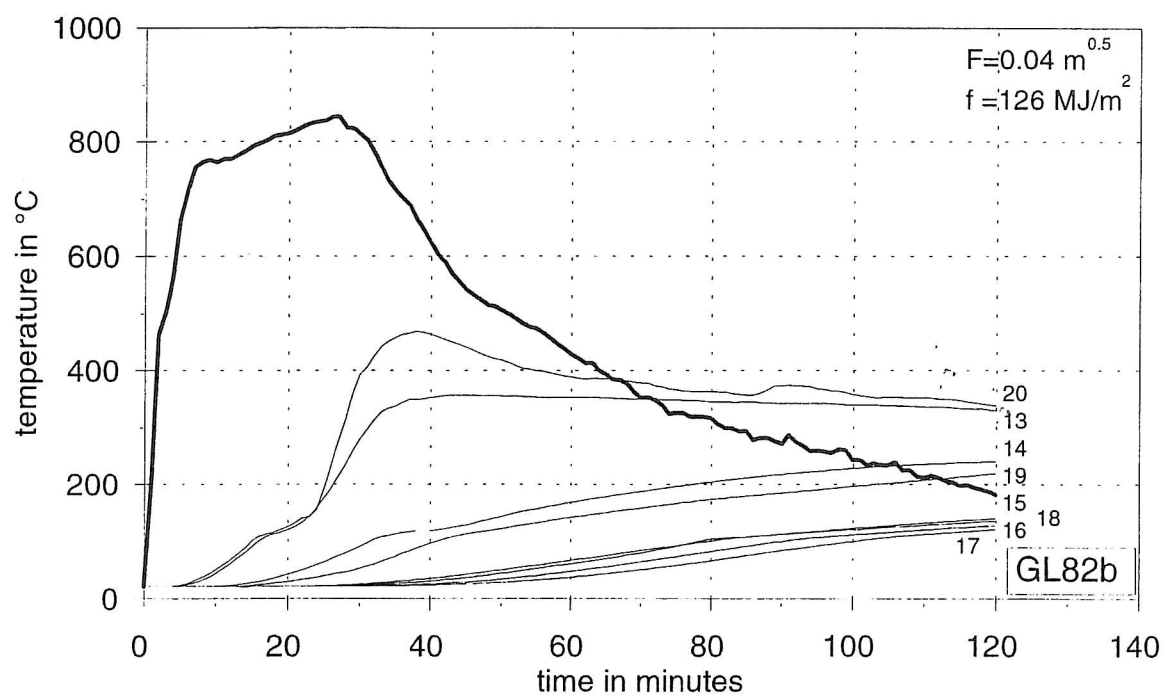
Relationship between fire load, charring depth and temperature inside the beams.



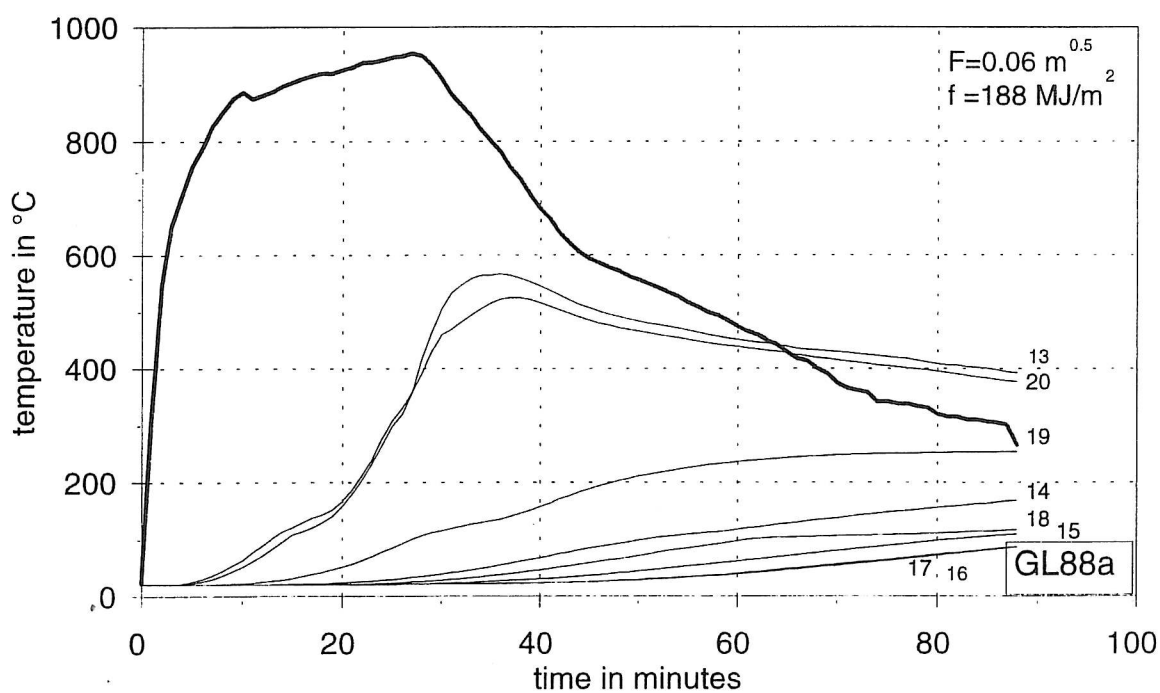
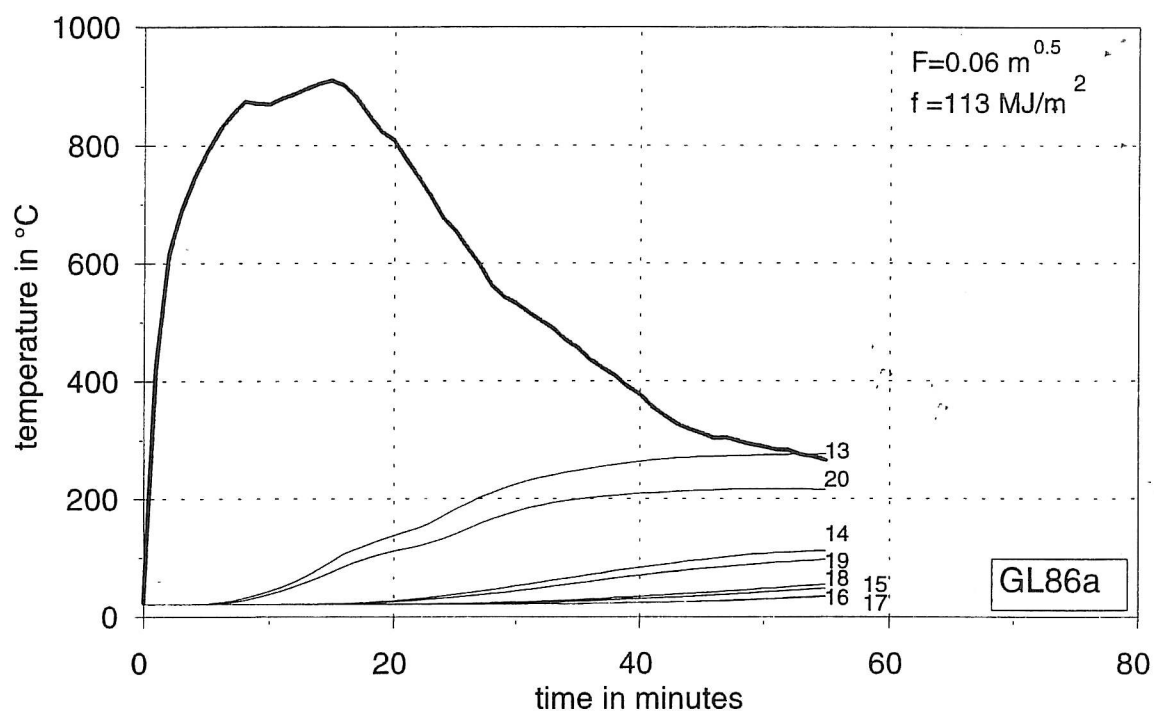
Relationship between fire load, charring depth and temperature inside the beams.



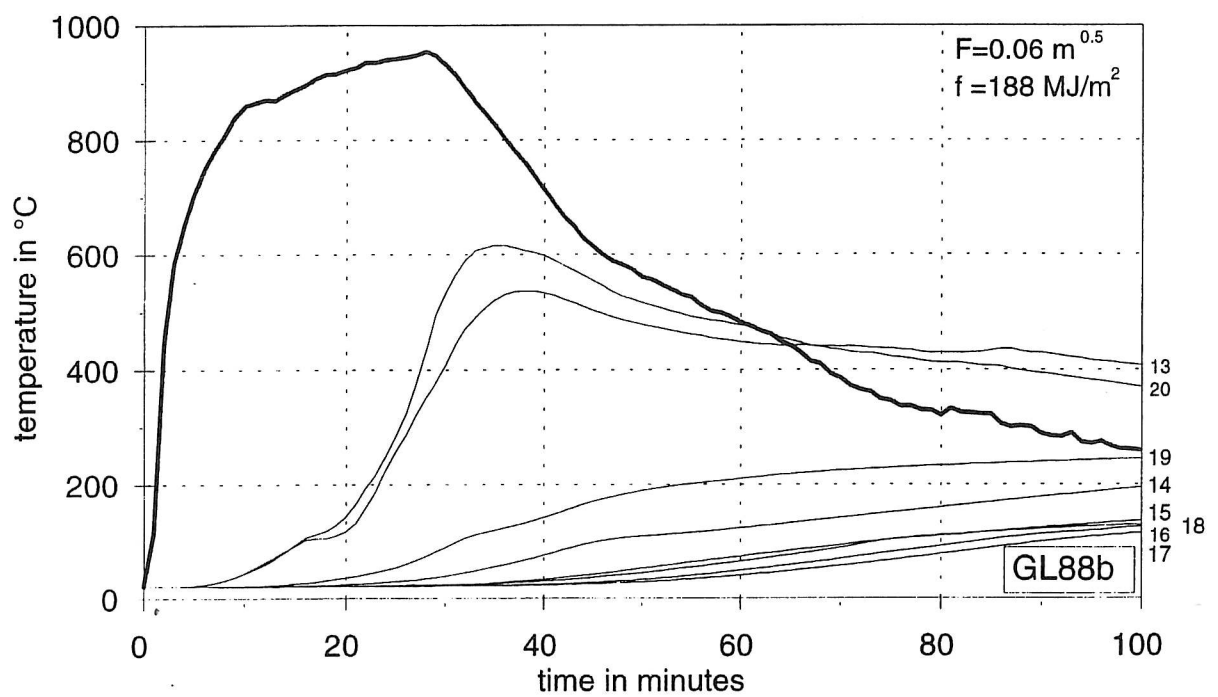
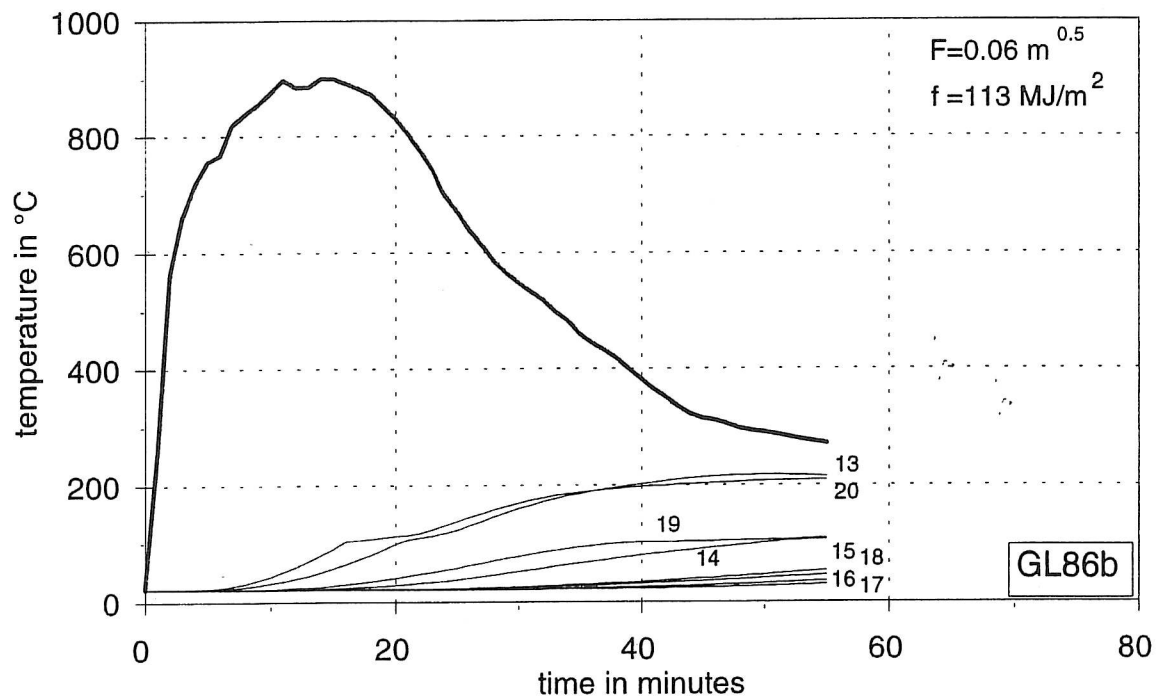
Relationship between fire load, charring depth and temperature inside the beams.



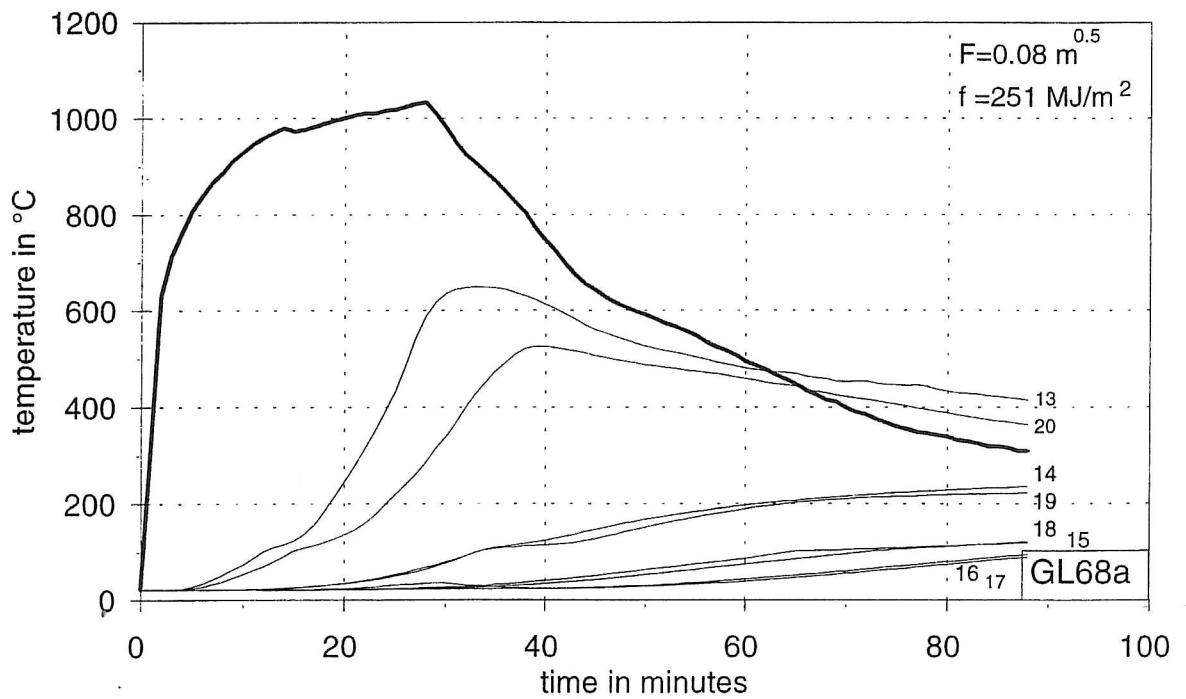
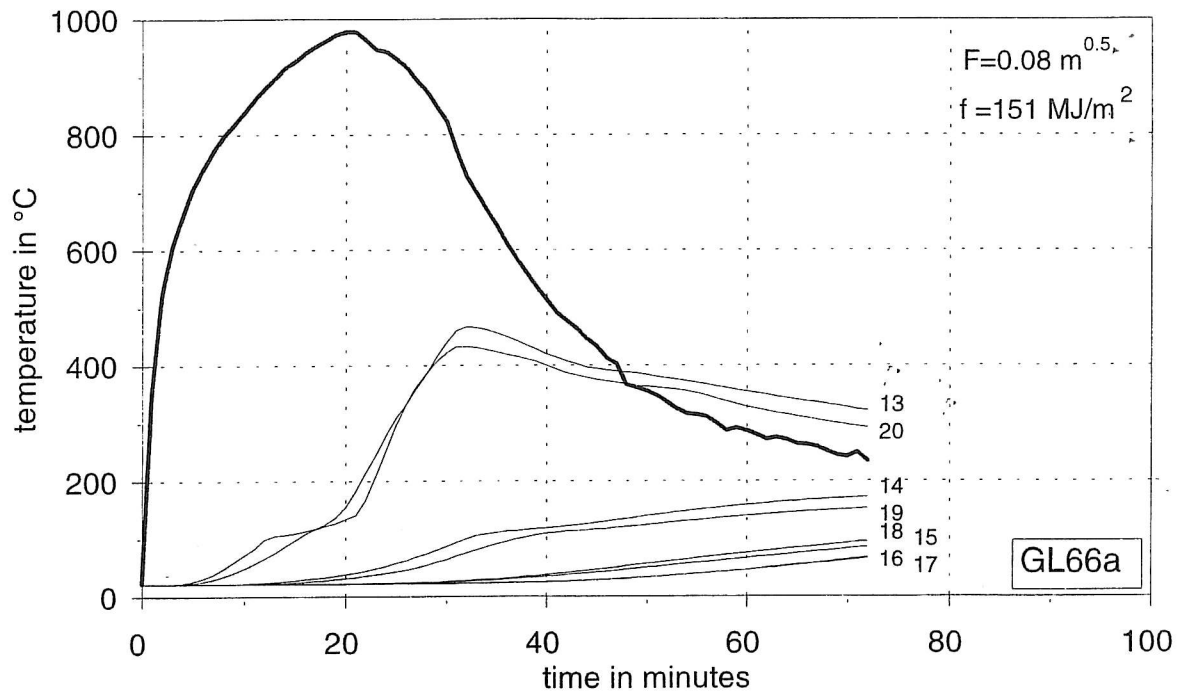
Relationship between fire load, charring depth and temperature inside the beams.



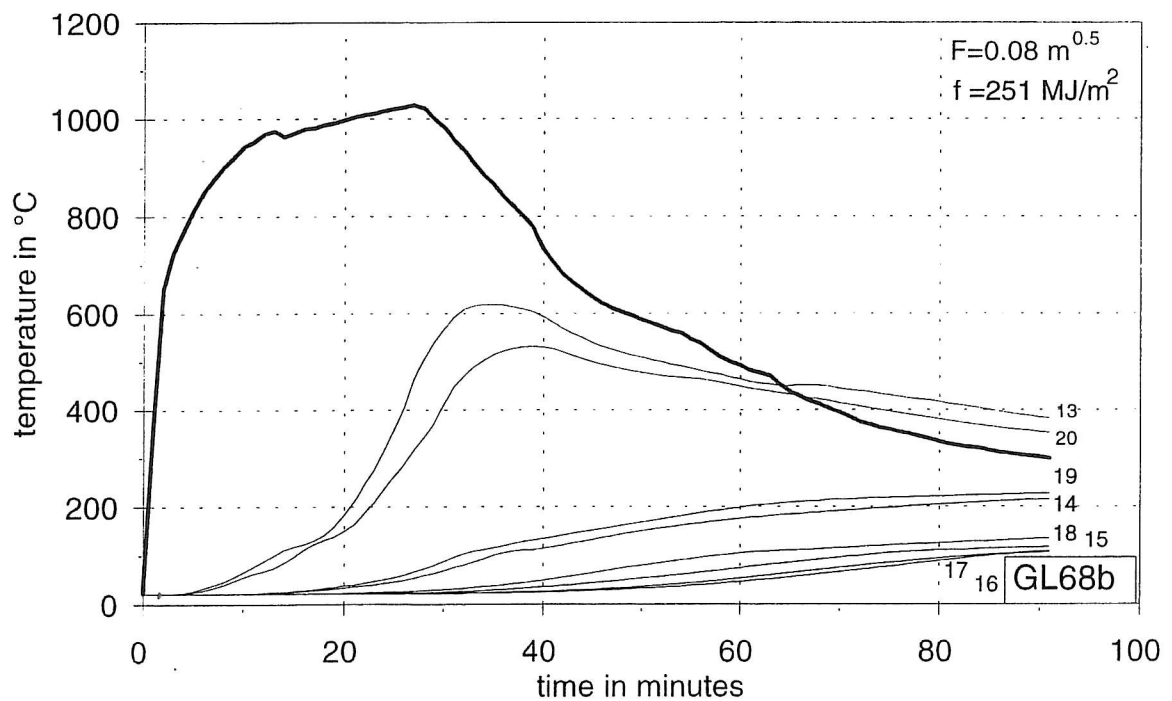
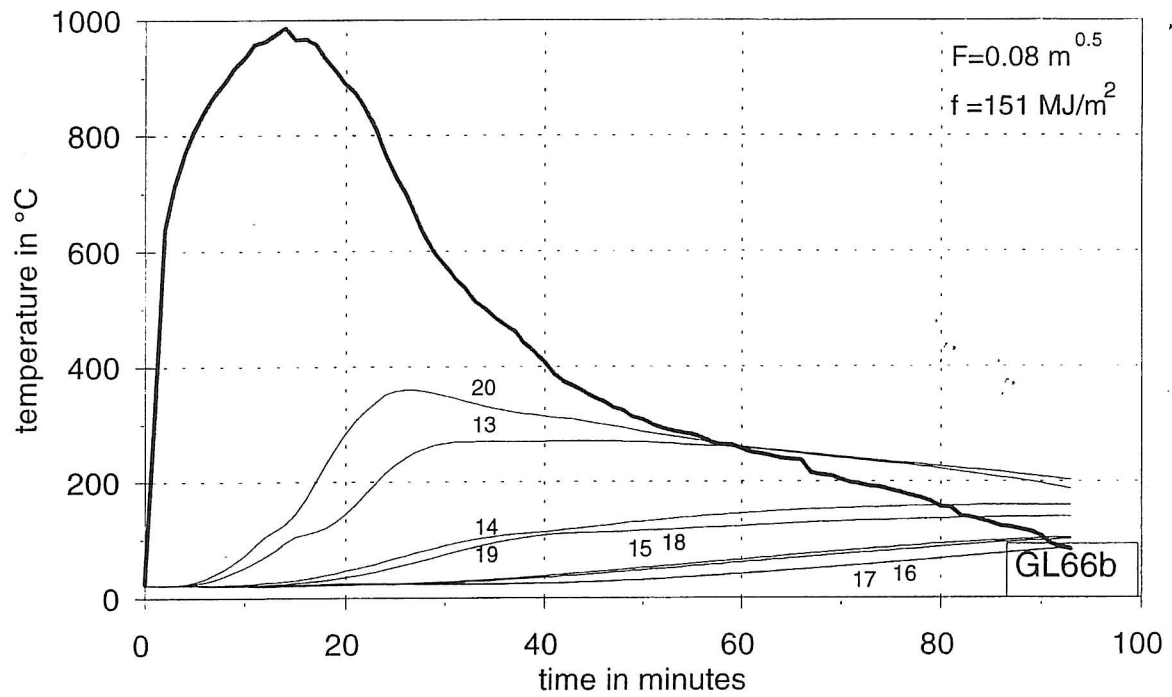
Relationship between fire load, charring depth and temperature inside the beams.



Relationship between fire load, charring depth and temperature inside the beams.



Relationship between fire load, charring depth and temperature inside the beams.



Relationship between fire load, charring depth and temperature inside the beams.

